Article

Trivalent recombinant protein vaccine induces cross-neutralization against XBB lineage and JN.1 subvariants: preclinical and phase 1 clinical trials

A list of authors and their affiliations appears at the end of the paper

The immune escape capacities of XBB variants necessitate the authorization of vaccines with these antigens. In this study, we produce three recombinant trimeric proteins from the RBD sequences of Delta, BA.5, and XBB.1.5, formulating a trivalent vaccine (Tri-Vac) with an MF59-like adjuvant at a 1:1:4 ratio. Tri-Vac demonstrates immunogenicity in female NIH mice, inducing cross-neutralization against various SARS-CoV-2 variants, including pre-Omicron and Omicron BA.2.75, BA.5, and XBB lineages. It elicits measurable antigen-specific T cell responses, germinal center B cell responses, and T follicular helper responses, effectively protecting against live Omicron XBB.1.16 challenges. Protective immunity is maintained long-term, with sustained neutralizing antibodies and T cell responses, as well as memory B cells and long-lived plasma cells observed by day 210 post-immunization. Tri-Vac also serves as a candidate booster for enhancing immunity after three doses of inactivated virus or mRNA vaccines. A phase 1 investigator-initiated trial was initiated to assess safety and immunogenicity in humans, focusing on the primary endpoint of adverse reactions within 7 days and key secondary endpoints including the geometric mean titers (GMTs) of serum neutralizing antibodies within 30 days and 6 months post-vaccination, as well as adverse events within 30 days and serious adverse events within 6 months post-vaccination. Preliminary data indicate Tri-Vac has good safety and immunogenicity, improving neutralization against multiple variants, including JN.1, in previously vaccinated individuals, highlighting its clinical potential for protecting against SARS-CoV-2 variants. The registration number of this clinical trial is ChiCTR2200067245.

Since its emergence in January 2020, severe acute respiratory coronavirus 2 (SARS-CoV-2) and its variants of concern (VOCs), including Alpha (B.1.1.7), Beta (B.1.351), Gamma (P.1), and Delta (B.1.617.2) have continued to spread, imposing a severe burden on global healthcare systems. In November 2021, the Omicron (B.1.1.529) variant emerged in South Africa, subsequently giving rise to various subvariants, including BA.1, BA.2, BA.2.75, BA.5, BF.7 and BQ.1.1[1–5]. By early 2023, recombinant XBB lineages with increased immune evasion abilities had emerged,

producing various descendant subvariants[6] such as XBB.1.5, XBB.1.16 (F486P)[7,8], EG.5 (with an additional F456L mutation), EG.5.1 (with F456L and Q52H mutations)[9–11], FL.1.5.1, HK.3 and HV.1[12]. Recently, subvariants originating from BA.2.86, including JN.1[13,14], KP.2, and KP.3, have also arisen and are competing globally.

Despite the World Health Organization (WHO) declaring the end of the emergency phase of the COVID-19 pandemic, the ongoing evolution and circulation of SARS-CoV-2 variants continue to threaten populations with repeated infections and complications such as Long-COVID. Vaccination remains an efficient strategy to protect against symptomatic infection, severe disease, and mortality. However, the emergence of XBB-lineages with remarkable immune evasion abilities has substantially impaired neutralization in individuals who have received monovalent or bivalent mRNA booster shots based on the pre-XBB-lineage sequences[2,15–17] or have experienced breakthrough infections with pre-XBB-lineage subvariants[1,6,16,18,19]. Consequently, the Food and Drug Administration (FDA) has approved several updated COVID-19 vaccines containing the antigen from XBB lineages, such as the XBB.1.5 monovalent mRNA vaccines by Moderna and Pfizer-BioNTech[20], and the adjuvanted XBB.1.5 spike protein vaccine by Novavax[21,22]. Preclinical and clinical studies have demonstrated that these updated vaccines can induce roust neutralization against XBB and JN.1 subvariants[21–26].

Nevertheless, vaccine development often lags behind the emergence of new variants, resulting in a continuous race between viral evolution and vaccine production. The unpredictable evolutionary directions of SARS-CoV-2 underscore the critical need for universal vaccines capable of increasing the magnitude and breadth of cross-neutralization response[27]. Although antigen derived from the XBB.1.5 subvariant can protect against several XBB-lineage-included Omicron variants[22,23,28], the neutralizing activities induced by XBB-lineages may be insufficient against pre-Omicron variants and other Omicron lineages due to distinct antigenic cartography between XBB-lineages and the cluster of other SARS-CoV-2 variants[29,30]. Therefore, assembling several key antigens from different SARS-CoV-2 strains represents a promising strategy for developing a multivalent vaccine capable of eliciting cross-neutralization responses.

This study extends our previous work, in which we reported the self-assembly of a trimeric protein, RBD$_{Delta}$-HR, by fusing the receptor binding domain (RBD) sequence from the Delta variant of SARS-CoV-2 to heptad-repeat sequences 1 and 2 (HR1 and HR2) within the spike S2 subunit[31]. Building upon this foundation, we have now engineered HR-fused RBD trimeric proteins specific to the BA.5 (RBD$_{BA.5}$-HR) and XBB.1.5 (RBD$_{XBB.1.5}$-HR) variants. Utilizing these proteins, we have formulated an adjuvanted trivalent vaccine, designated as Tri-Vac, which incorporates RBD$_{Delta}$-HR, RBD$_{BA.5}$-HR, and RBD$_{XBB.1.5}$-HR in an antigenic ratio of 1:1:4. Tri-Vac was designed to elicit a cross-neutralizing immune response against a spectrum of SARS-CoV-2 variants, encompassing both pre-Omicron strains such as the prototype and Delta, as well as Omicron subvariants including BA.2.75, BA.5, and its derivatives (BF.7, BQ.1, BQ.1.1), and the XBB lineage (XBB, XBB.1.5, XBB.1.16). Vaccination of Tri-Vac in mice results in antigen-specific cellular immune response, germinal center response, and long-lasting humoral and cellular immunity. Notably, heterologous immunization with Tri-Vac rescued the neutralizing activities against Omicron variants that include XBB, in mice previously having received three doses of either prototypic inactivated vaccine or mRNA vaccine based on the pre-Omicron sequences. In addition, Tri-Vac provides adequate protection against the challenge of live XBB.1.16 subvariant infection in vivo. In human participants, Tri-Vac demonstrated acceptable safety and a pronounced boosting effect, improving neutralizing antibody responses against JN.1 and XBB-lineage variants. These results demonstrate the potential of Tri-Vac as a universal COVID-19 vaccine candidate for clinical application.

Results

Characterization of the recombinant RBD$_{BA.5}$-HR and RBD$_{XBB.1.5}$-HR

Based on the fact that peptides harboring the spike HR1 and HR2 could automatically assemble into a 6-helix bundle structure[32,33], we previously reported the development of a self-assembled trimeric protein by directly linking an RBD sequence derived from the Delta variant with HR1 and an HR2 sequences in a tandem manner[31]. In this study, we utilized this design feature and successfully produced trimeric proteins, namely RBD$_{BA.5}$-HR and RBD$_{XBB.1.5}$-HR, by linking the RBD sequence (amino acids V320-G545) of the BA.5 and XBB.1.5 variants, respectively, with HR1 (amino acids L916-L966) and HR2 (amino acids K1157-L1203) sequences (Fig. 1a-b). The designed protein sequence incorporates a GP67 signal peptide for protein secretion, a Trx tag for protein folding, a 6×His tag for protein purification, and an enterokinase (EK) cleavage site for tag removal, all in a tandem arrangement at N-terminus (Fig. 1b). Molecular modeling predicted that this design facilitates the clustering of three RBD molecules on one side and the stacking of HR1/HR2 helices on the other side, creating a bouquet-like shape (Fig. 1c). The recombinant proteins were expressed using Bac-to-Bac Baculovirus Expression System and purified to a high level of homogeneity, as described previously[31]. SDS-PAGE analysis confirmed successful cleavage at the EK site to remove the Trx-His-EK tag, with a molecular weight of -16 kDa (Supplementary Fig. 1a). N-terminal sequencing verified the absence of the Trx-His-EK tag in the recombinant RBD-HR proteins after cleavage by enterokinase (Supplementary Fig. 1c). The trimeric structure of the purified proteins was indicated by an elution peak at approximately 13 ml on a Superdex 200 increase column (Fig. 1d), and the eluted recombinant proteins were confirmed by western blotting (Supplementary Fig. 1b). To further validate the structure of RBD$_{BA.5}$-HR and RBD$_{XBB.1.5}$-HR, negative-staining transmission electron microscopy (TEM) was performed, revealing the trimeric, bouquet-like structure of these recombinant proteins (Fig. 1e). TEM images were annotated with red arrows to indicate representative protein particles, which were then selected for 2D classifications, and the results showed corroborated the bouquet-like structure, with each RBD and the HR-trimer resembling a petal, thus confirming the clustering of three RBD proteins. These results strongly demonstrate the successful production of trimeric RBD$_{BA.5}$-HR and RBD$_{XBB.1.5}$-HR proteins, which are structurally consistent with the intended design.

Tri-Vac elicited cross-neutralization response against multiple SARS-CoV-2 variants

To explore the potential of a multi-antigen approach to induce cross-neutralization against diverse SARS-CoV-2 variants, a trivalent vaccine was formulated, integrating RBD$_{Delta}$-HR, RBD$_{BA.5}$-HR, and RBD$_{XBB.1.5}$-HR antigens in a 1:1:4 ratio, hereinafter referred to as Tri-Vac (Fig. 2a). Female NIH mice were administered 10 μg of Tri-Vac, adjuvanted with MF59-like formulation, via the intramuscular route, following a prime-boost regimen with a 21-day interval, as shown in Fig. 2a. Control groups received equivalent doses of adjuvanted monomeric antigens: RBD$_{Delta}$-HR, RBD$_{BA.5}$-HR, and RBD$_{XBB.1.5}$-HR. Binding antibody assays revealed that all adjuvanted protein antigens could elicit high levels of RBD-specific IgG, with endpoint titers exceeding 10^6 post-immunization (Fig. 2b).

Pseudovirus assays were then performed to determine the neutralizing activities in serum samples (Fig. 2c, d). Consistent with previous studies[6,8], the neutralizing capacities induced by the pre-Omicron variant-based antigen (RBD$_{Delta}$-HR) were significantly impaired by Omicron variants, particularly those within the XBB lineages. When compared to Delta pseudovirus neutralization, the geometric mean titers (GMTs) of 50% neutralization against BA.5 and

XBB.1.5 induced by RBD$_{Delta}$-HR were decreased by 10.1- and respectively. The RBD$_{BA.5}$-HR antigen elicited neutralizing antibodies against several pre-Omicron variants, yet faced substantial impairment against multiple XBB subvariants, aligning with the known immune evasion properties of the XBB lineage[2,15-17,19]. For instance, in the group receiving the RBD$_{BA.5}$-HR antigen, the GMTs against XBB, XBB.1.5, and

XBB.1.16 were decreased by 23.5-, 19.9-, and 35.8-fold, respectively, when compared to BA.5 pseudovirus. The RBD$_{XBB.1.5}$-HR protein is able to elicit neutralizing responses against multiple XBB-lineage Omicron variants. However, neither RBD-HR derived from BA.5 nor XBB.1.5 induced enough cross-neutralizing antibodies against pre-Omicron variants (prototype and Delta strains) (Fig. 2c), emphasizing the need
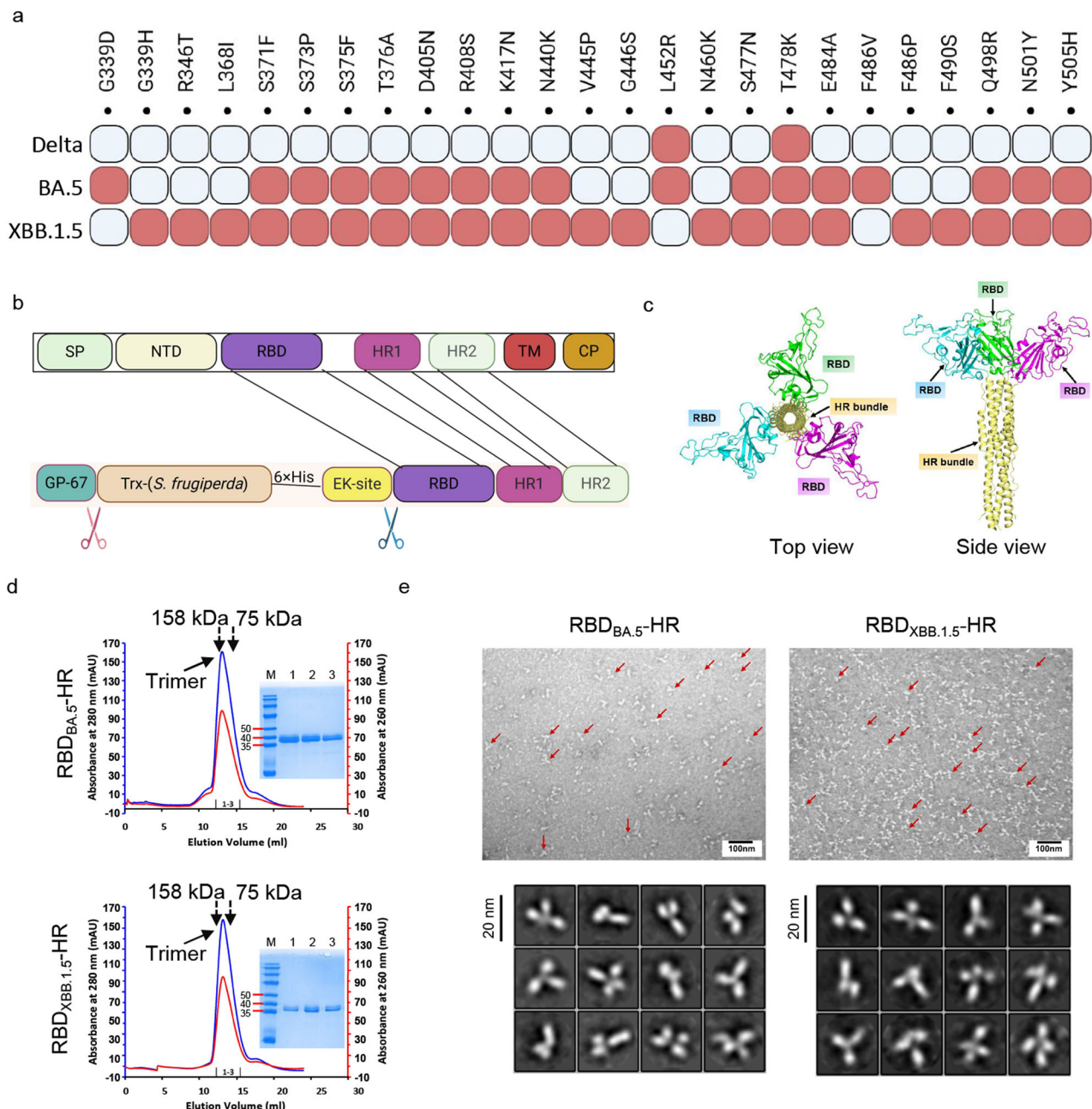

Fig. 1 | Characterization of the recombinant trimeric RBD$_{BA.5}$-HR and RBD$_{XBB.1.5}$-HR proteins. a The schematic representation of mutations in receptor-binding domain (RBD) proteins of SARS-CoV-2 Delta, BA.5 and XBB.1.5 variants. **b** The schematic representation of the SARS-CoV-2 spike protein and the design of trimeric RBD-HR proteins. The RBD$_{BA.5}$-HR and RBD$_{XBB.1.5}$-HR proteins include an RBD (320-545 aa) derived from the BA.5 or XBB.1.5 variants and HR1 (916-966 aa) and HR2 (1157-1203 aa) domain in subunit S2 of the spike protein. In addition, the designed protein sequence is fused at its N-terminal in a tandem manner with the sequences of a GP67 signal peptide for protein secretion, a Trx tag for protein folding, a 6×His tag for the protein purification and an enterokinase (EK) cleavage site for tag removal. SP signal peptide; NTD N-terminal domain; RBD receptor binding domain; HR1 and HR2: heptad repeats 1 and 2; TM: transmembrane

domain; CP: cytoplasmic domain. The schematics in (**a**, **b**) were Created in BioRender. Wang, Y. (2023) BioRender.com/i76n600. **c** Molecular model from top view and side view of the trimeric RBD-HR protein with a bouquet-like shape. **d** A representative elution chromatograph of the RBD$_{BA.5}$-HR and RBD$_{XBB.1.5}$-HR proteins on a calibrated Superdex Increase 200 column. The SDS-PAGE of the eluted recombinant proteins was shown. Clearly shown is that both proteins are eluted around 13 ml, indicating the formation of RBD-HR trimers. **e** Transmission electron microscopy (TEM) images of the RBD$_{BA.5}$-HR and RBD$_{XBB.1.5}$-HR protein with a bouquet-like shape. The top 2 panels were negative-staining TEM images of the indicated RBD-HR protein, and the representative protein particles were marked with red arrows. The bottom two panels showed the reconstructed 2D image of the protein particles. The scale bar represents 100/20 nm in (**e**).
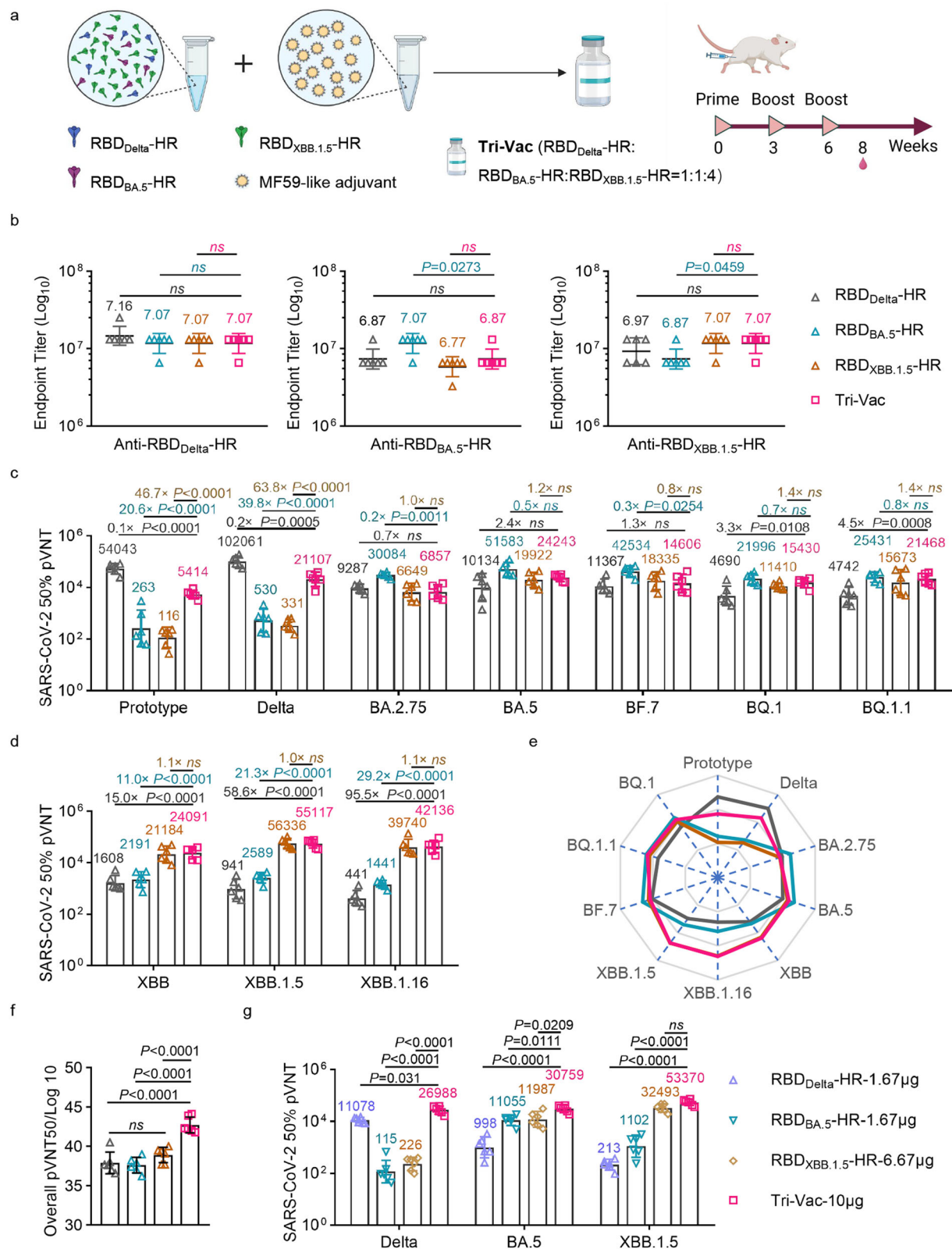
to develop universal COVID-19 vaccines by incorporating multiple antigens derived from both pre-Omicron and Omicron variants.

It is worth noting that Tri-Vac, incorporating three RBD-HR antigens derived from Delta, BA.5, and XBB.1.5, induced a broad-spectrum of neutralizing antibodies against a panel of SARS-CoV-2 pseudoviruses. Although the GMTs for pre-Omicron variants in the Tri-Vac group were lower than those in the RBD$_{Delta}$-HR group, they were

significantly higher than those in the RBD$_{BA.5}$-HR and RBD$_{XBB.1.5}$-HR group. For example, the GMTs of neutralizing antibodies against Delta pseudovirus in the RBD$_{BA.5}$-HR and RBD$_{XBB.1.5}$-HR groups were determined to be 530 and 331, respectively, while the GMTs in the Tri-Vac group were 39.8- and 63.8-fold higher than GMTs in that two groups, respectively, and could reach 21107 (Fig. 2c). In addition, Tri-Vac rescued the impaired neutralization against XBB-lineages subvariants,

Fig. 2 | Tri-Vac elicits cross-neutralization response against XBB lineages-included SARS-CoV-2 variants. a The female NIH mice were intramuscularly immunized three times with 10 μg of MF59-like adjuvant-formulated trivalent vaccine (Tri-Vac) containing RBD$_{Delta}$-HR, RBD$_{BA.5}$-HR and RBD$_{XBB.1.5}$-HR antigens with a ratio of 1:1:4. The mice immunized with 10 μg of adjuvanted RBD$_{Delta}$-HR, RBD$_{BA.5}$-HR, or RBD$_{XBB.1.5}$-HR protein were used as control. The schematic in (**a**) was created in BioRender. Wang, Y. (2024) BioRender.com/x72d484. **b** Endpoint titers of antigen-specific binding antibodies in serum samples from immunized mice. Sera neutralizing antibody titers against (**c**) pre-Omicron (prototype, Delta), Omicron BA.2.75, BA.5, BF.7, BQ.1, BQ.1.1, and (**d**) XBB-lineage variants (XBB, XBB.1.5 and XBB.1.16) pseudoviruses. **e** The radar chart was generated from the data of Log10 GMTs in (**c, d**) to reveal the tropism of neutralizing antibody response induced by Tri-Vac and each individual antigen. **f** The summation of Log10 50% neutralization titers against all pseudovirus in (**c, d**) for each immunized mouse in each group.

g Female NIH mice were immunized with 10 μg of Tri-Vac or individual antigenic components of Tri-Vac, including 1.67 μg of RBD$_{Delta}$-HR, 1.67 μg of RBD$_{BA.5}$-HR, and 6.67 μg of RBD$_{XBB.1.5}$-HR, respectively, and the sera neutralization against pseudovirus were detected to determine whether the three antigens in Tri-Vac influence each other when inducing humoral immune response. Serum samples in (**b–d**) and (**g**) were collected on day 14 after the final immunization. $n = 6$ mice per group in (**b–g**). Data are presented as geometric mean values with 95% confidence intervals (CI) in (**b–d**) and (**g**) and as mean values with SD in (**f**). P-values in (**b**) were performed by ordinary One-way ANOVA analysis followed by Dunnett's multiple comparisons test after the Log10 transformation, and in (**c, d**, and **g**) were performed by Two-way ANOVA analysis followed by Dunnett's multiple comparisons test after the Log10 transformation, and (**f**) were performed by ordinary One-way ANOVA analysis followed by Tukey's multiple comparisons test. ns not significant.

with a 58.6- and 21.3-fold improvement in GMTs against XBB.1.5 pseudovirus compared to the RBD$_{Delta}$-HR and RBD$_{BA.5}$-HR groups, respectively. For BA.2.75, BA.5, and its descendants (BF.7, BQ.1, and BQ.1.1), the Tri-Vac vaccinated mice exhibited neutralizing antibody levels slightly lower than those with RBD$_{BA.5}$-HR but higher than those with antigens from Delta and XBB.1.5 sequences (Fig. 2c, d).

A radar chart was constructed to visualize the neutralizing response tropism induced by Tri-Vac and individual antigens (Fig. 2e), illustrating that each antigen preferentially neutralized its homologous variant. To be specific, the neutralization induced by RBD$_{Delta}$-HR antigen (black line) was well response to pre-Omicron variants but impaired by all Omicron variants, which was manifested by the line being close to the prototype and Delta virus and away from the Omicron variants, especially XBB-lineages. Conversely, RBD$_{BA.5}$-HR protein (blue line) is unable to induce strong neutralization against pre-Omicron and XBB-lineage variants, while RBD-HR antigen derived from XBB.1.5 (claybank line) induced a response against multiple Omicron subvariants with minimal protection against pre-Omicron variants. The Tri-Vac, represented by the pink line, displayed a more uniform polygon, indicating cross-neutralization against multiple variants. We then summed, for each immunized mouse, the titers of 50% neutralizing antibody against all pseudoviruses (pVNT50) for each group and found that the total pVNT50 in the Tri-Vac group surpassed those of the individual antigen groups (Fig. 2f).

Two additional trivalent vaccines, with adjusted RBD$_{Delta}$-HR, RBD$_{BA.5}$-HR, and RBD$_{XBB.1.5}$-HR antigen ratios of 1:1:1 and 1:2:3, were prepared and evaluated (Supplementary Fig. 2). Both vaccines induced similar cross-neutralization responses. However, Tri-Vac, with a 1:1:4 antigen ratio, exhibited the most potent neutralization against XBB lineages, leading to its selection for further studies.

In the next set of experiments, mice were immunized with each of the antigenic components (1.67 μg of RBD$_{Delta}$-HR, 1.67 μg of RBD$_{BA.5}$-HR, or 6.67 μg of RBD$_{XBB.1.5}$-HR) of the Tri-Vac. We found that the titers of neutralizing antibodies induced by the Tri-Vac were comparable to or exceeded those induced by the individual components against their corresponding pseudoviruses (Fig. 2g). For instance, the GMT against Delta pseudovirus in the group receiving 1.67 μg of RBD$_{Delta}$-HR was determined to be 11078, whereas in the Tri-Vac group, it was to be 26988. Similar results were observed for 1.67 μg of RBD$_{BA.5}$-HR and 6.67 μg of RBD$_{XBB.1.5}$-HR, indicating that the three antigens in Tri-Vac will not influence each other when inducing humoral immune response.

Tri-Vac induced robust cellular immune and germinal center responses

Cellular immune responses involving CD4$^+$ and CD8$^+$ T cell responses play a crucial role in protecting against SARS-CoV-2 infection[34,35]. In this study, the capacity of Tri-Vac to activate antigen-specific T-cell responses was evaluated. Splenic lymphocytes, harvested 56 days post-initial immunization, were isolated and stimulated with peptide pools that overlapped the SARS-CoV-2 spike protein. To investigate whether the cellular immunity induced by Tri-Vac can respond to

antigens from multiple variants, three distinct spike peptide pools, representative of wildtype, BA.5, and XBB.1.5 sequences, were utilized. Intracellular cytokine staining (ICS) was employed to assess the secretion of IFN-γ and TNF by CD4$^+$ and CD8$^+$ T cells upon stimulation. The results showed a scarcity of IFN-γ- and TNF-secreting T cells in groups administered PBS or MF59-like adjuvant alone, contrasting with the pronounced increase in the proportion of spike-specific memory CD4$^+$ and CD8$^+$ T cells in Tri-Vac-vaccinated mice, which produced these cytokines in response to stimulation (Fig. 3a–d). These results indicated the induction of potent cellular immune responses against a variety of SARS-CoV-2 variants by Tri-Vac in mice.

The induction of robust germinal center B (GC B) and T follicular helper (Tfh) cell responses is imperative for the establishment of long-term protective immunity against SARS-CoV-2 infection[36,37]. The impact of Tri-Vac on the emergence of GC B (CD19$^+$GL7$^+$CD95$^+$)[38] and Tfh (CD4$^+$CXCR5$^+$PD-1$^+$)[39] cells within spleen tissues and inguinal lymph nodes was therefore examined (Fig. 3e, f). As expected, immunization with Tri-Vac significantly augmented the GC B and Tfh responses, manifested by the elevated frequencies of these cells in the lymph nodes and spleen. To identify antigen-specific GC B cells, cells from lymph nodes were incubated with recombinant RBD protein from the XBB.1.5 subvariant, revealing the presence of RBD-specific GC B cells exclusively in the Tri-Vac group. These outcomes suggest that Tri-Vac vaccination induces potent Tfh and GC B cell responses within the germinal centers.

Tri-Vac provided long-term protective humoral and cellular immunity

Given the persistent nature of the COVID-19 pandemic, the establishment of long-term protective immunity is essential for population-wide defense. A sustained antibody response is a critical marker for safeguarding against recurrent SARS-CoV-2 infections. To assess the capacity of Tri-Vac to elicit a durable humoral immune response, we measured the levels of serum-neutralizing antibodies at extended intervals following immunization completion. The results revealed that neutralizing antibody titers against a range of pseudoviruses, including BA.5, BQ.1.1, XBB.1.5, XBB.1.6, XBB.1.16, XBB.1.9.1, XBB.2.3, and EG.5.1, were comparatively elevated on days 70, 100, and 210 post-prime immunization. Although a decline was observed in antibody levels on day 210 compared to day 70, the GMTs for these viruses remained above 3500, indicating the Tri-Vac is able to induce the persistent antibody responses (Fig. 4a). Furthermore, the induction of antibody-secreting cells (ASCs) in bone marrow and spleen tissues was evaluated on day 210 post-vaccination, with a significant increase in RBD-specific ASCs observed in the Tri-Vac group relative to the PBS group (Fig. 4b, c).

B cell activation, which can lead to either extrafollicular (EF) or germinal center (GC) responses, is integral to the production of somatically mutated memory B cells (MBCs) and long-lived plasma cells (LLPCs), both of which are vital for the maintenance of long-term antibody production[40,41]. To determine if the long-term antibody
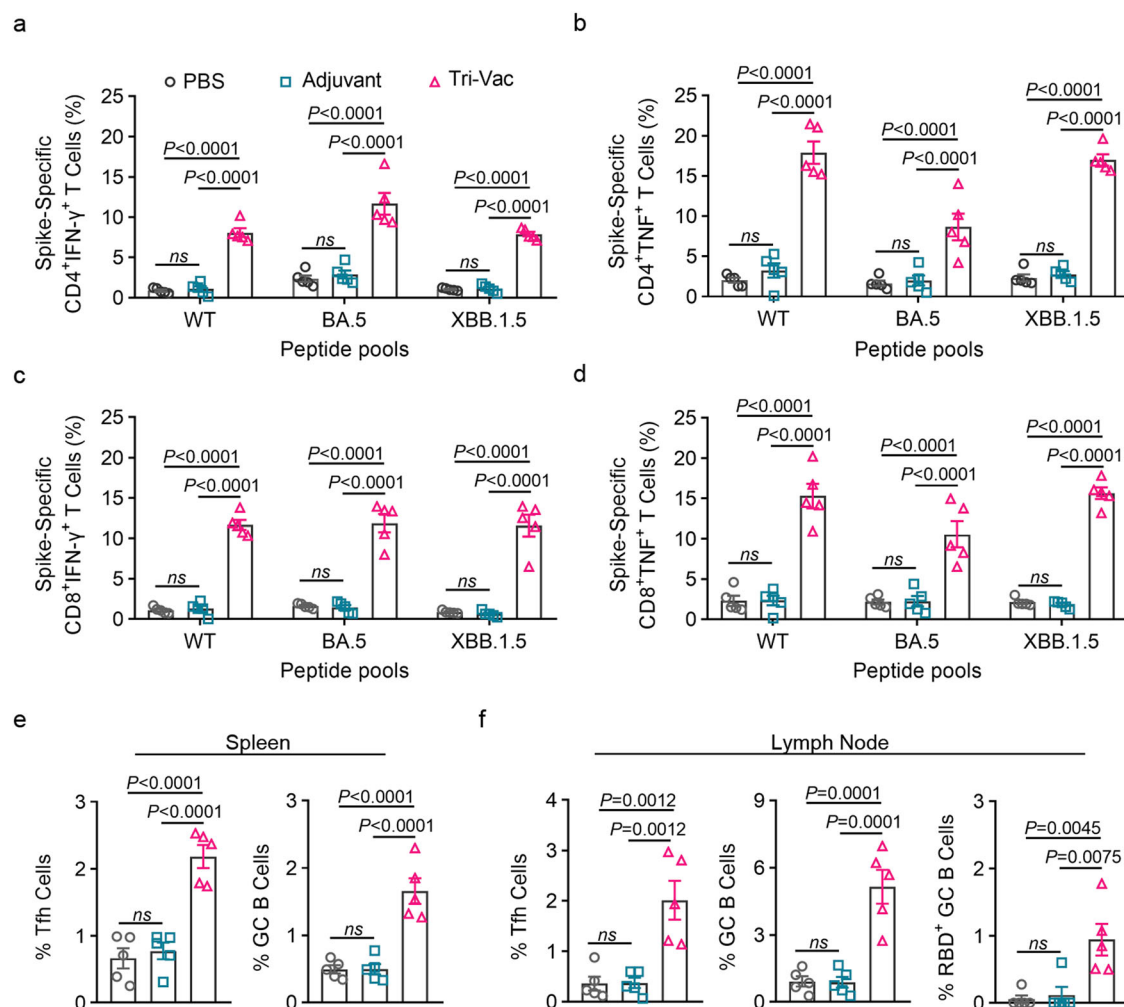
Fig. 3 | Tri-Vac induces strong T cell immune response in vivo. The percentages of IFN-γ- and TNF-secreting CD44+CD4+ (**a, b**) and CD44+CD8+ (**c, d**) memory T cells in spleen tissues after stimulation with three peptide pools covering spike protein of wildtype, BA.5, and XBB.1.5 variant, respectively. **e** The frequencies of T follicular helper (Tfh) cells (CD4+CXCR5+PD-1+) and germinal center B (GC B) cells (CD19+GL7+CD95+) in spleen tissues. **f** The frequencies of Tfh, GC B, and RBD-specific GC B cells in inguinal lymph nodes. Spleen and lymph nodes were collected on day 56 after the first vaccination. $n = 5$ mice per group in (**a**–**f**). Data are presented as mean with SEM in (**a**–**f**). P values in (**a**–**d**) were performed by Two-way ANOVA analysis followed by Tukey's multiple comparisons test, and (**e**, **f**) were conducted by One-way ANOVA analysis followed by Tukey's multiple comparisons test. ns, not significant.

responses induced by Tri-Vac are linked to the generation of MBCs and LLPCs, we quantified these cell populations. In line with our expectations, the frequencies of MBCs in lymph nodes and spleen (Fig. 4d, e), as well as LLPCs in bone marrow (Fig. 4f), were markedly elevated on day 210 following the initial vaccination.

In addition, we assayed the frequencies of splenic antigen-specific T cells on day 210 after the first immunization, and the results exhibited a relatively large number of IFN-γ-secreting CD4+ and CD8+ T cells after stimulation with XBB.1.5 spike protein peptide pools (Fig. 4g), suggesting the persistence of cellular immunity conferred by Tri-Vac.

Tri-Vac as a heterologous booster improved neutralizing capacity against XBB lineages-included SARS-CoV-2 variants

Inactivated virus and mRNA-based COVID-19 vaccines have been granted global approval for use[42,43]. Nevertheless, the neutralizing actives induced by these previously marketed inactivated and mRNA vaccines, including the bivalent mRNA vaccine containing the BA.5 sequence, have been extensively impaired by XBB lineage subvariants[1,2,15–17,44,45]. Moderna and Pfizer/BioNTech have updated their mRNA vaccine antigenic sequences to include the full-length spike protein of XBB.1.5[20], which has been shown to induce robust neutralizing antibodies against XBB and JN.1 subvariants[23]. Despite

this, some studies propose that recombinant protein-based vaccines could serve as effective heterologous boosters following initial inactivated or mRNA vaccinations[46–48]. In light of this, we explored the potential of Tri-Vac to function as a heterologous booster in a sequential immunization strategy aimed at protecting against XBB-inclusive variants.

Mice were first intramuscularly injected with three doses of either a prototypic SARS-CoV-2 inactivated vaccine or an mRNA vaccine based on the sequence of full-length spike protein of Delta variant at 0, 2, 6 weeks, followed by a fourth booster dose with either an inactivated vaccine (IV×3 > IV), an mRNA vaccine (mRNA×3 > mRNA), or Tri-Vac (IV×3 > Tri-Vac, and mRNA×3 > Tri-Vac), at 16 weeks since the first immunization (Fig. 5a, d). Consistent with our expectation, authentic virus neutralization assays demonstrated that Omicron variants, particularly XBB.1.16, significantly escaped the neutralizing antibodies induced by homologous vaccination with inactivated and mRNA vaccines (Fig. 5b, e). However, heterologous immunization with Tri-Vac as the fourth booster significantly rescued the levels of neutralizing antibodies against XBB lineages-included SARS-CoV-2 variants. Specifically, the GMTs of 50% neutralization in the heterologous vaccination group against Delta, BA.2.75, BA.5.2.48 and XBB.1.16 viruses were improved by 10.6-, 12.1-, 32.0-, and 55.4-fold, respectively, compared to
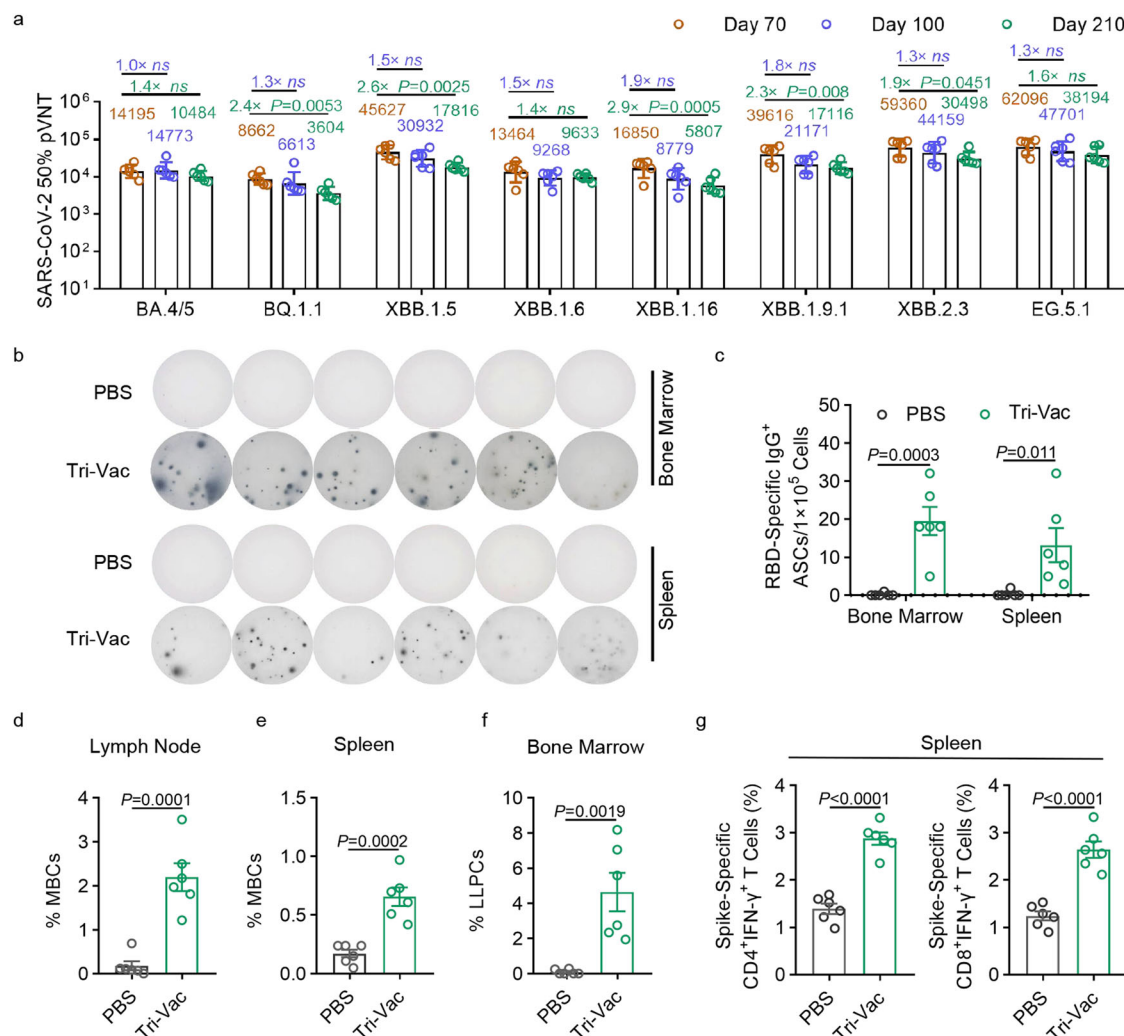
Fig. 4 | Tri-Vac provides long-term protective immunity in vivo. a Female NIH mice were intramuscularly injected three times with 10 µg of Tri-Vac at 0, 3, and 6 weeks, the serum samples were collected on days 70, 100, and 210 after the first immunization. Immunized mice were then sacrificed for sample collection on day 210 to determine the long-lasting immune responses. Neutralizing antibodies in serum samples against a variety of pseudoviruses were determined. The representative images (**b**) and quantitative analysis (**c**) of RBD-specific IgG antibody-secreting cells (ASCs) in the bone marrow and spleen tissues. The percentages of memory B cells (MBCs) in lymph nodes (**d**) and spleen (**e**). **f** The percentage of long-lived plasma cells (LLPCs) in the bone marrow. **g** The percentages of splenic IFN-γ-secreting CD44$^+$CD4$^+$ and CD44$^+$CD8$^+$ memory T cells after stimulation with spike peptide pools covered spike proteins of XBB.1.5 variant. $n = 6$ mice per group in (**a–g**). Data are presented as geometric mean values with 95% CI in (**a**), and presented as mean with SEM in (**c–g**). *P* values in (**a**) were conducted by Two-way ANOVA analysis followed by Tukey's multiple comparisons test after the Log10 transformation, and in **c** were conducted by Two-way ANOVA analysis followed by Sidak's multiple comparisons tests, and in (**d–g**) were performed by two-tailed Unpaired Student's *t*-tests. ns not significant.

the homologous inactivated vaccine group (Fig. 5b), and enhanced by 1.5-, 5.3-, 12.1- and 32.0-fold, respectively, compared to the group with homologous immunization with mRNA vaccine (Fig. 5e). Pseudovirus neutralization assays further confirmed the neutralizing capacities of the sera (Fig. 5c, f). Although XBB lineage variants showed extensive resistance to neutralization induced by inactivated and mRNA vaccines, a single dose of Tri-Vac as a booster rescued the neutralizing activities against all XBB subvariants (XBB, XBB.1.5, XBB.1.6, XBB.1.9.1, XBB.1.16, and XBB.2.3). Specifically, the GMT of 50% neutralization against XBB, XBB.1.5, XBB.1.6, XBB.1.9.1, XBB.1.16, XBB.2.3 subvariants reached 7622, 39622, 21859, 23857, 18738, and 23690, respectively, in the group that received three doses of inactivated vaccine followed one dose of Tri-Vac (Fig. 5c), and reached 24443, 35395, 32489, 31791, 20283 and 38744, respectively, in the group that received the mRNA vaccine with a heterologous booster of Tri-Vac (Fig. 5f). These results demonstrate that heterologous vaccination with Tri-Vac elicits robust neutralizing capacities to protect against XBB lineages-included variants.

In addition to the antibody response, heterologous immunization with Tri-Vac enhanced the germinal center and cellular immune response, as indicated by higher frequencies of Tfh and GC B cells in lymph nodes and spleen tissues (Fig. 5g, h) and IFN-γ and TNF-secreting T memory cells in spleen tissues after stimulation with spike peptide (Fig. 5i, j). These results indicated that the Tri-Vac protein vaccine is able to serve as a candidate booster shot for heterologous immunization following inactivated and mRNA vaccinations.

Tri-Vac provided effective protection against live XBB.1.16 Omicron virus challenge

The efficacy of Tri-Vac against live virus infection was evaluated in vivo using the XBB.1.16 variant, selected due to its global prevalence at the time of the experiment. NIH mice were immunized with three doses of either a low dose (5 µg) or a high dose (10 µg) of Tri-Vac vaccine, while mice immunized with adjuvant alone served as controls. Before the viral challenge, serum samples were collected to evaluate the neutralization against authentic viruses. Consistent with the results of
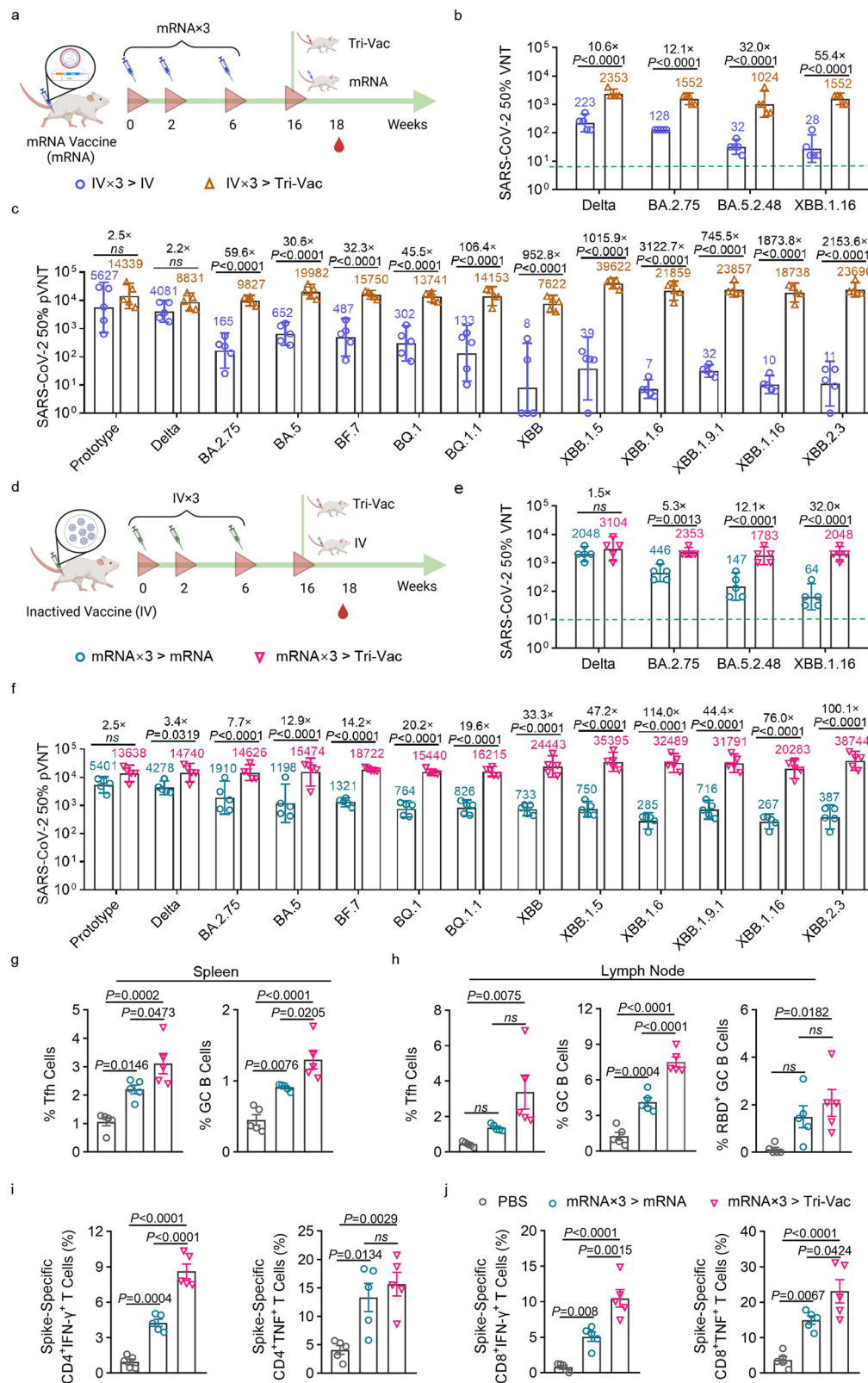
pseudovirus neutralization assays, Tri-Vac elicited broad-spectrum neutralization capacities against XBB-included SARS-CoV-2 variants. The GMTs for 50% neutralization against XBB.1.16 were 1149 in the low-dose group and 1825 in the high-dose group, and the neutralization induced by the Tri-Vac vaccine was effective against authentic Delta, BA.2.75, and BA.5.2.48 viruses (Fig. 6a). Although the GMTs in the high-dose group were modestly higher than in the low-dose group, no

statistically significant differences were observed in neutralizing anti-body levels against live viruses, with the exception of the Delta variant.

The mice immunized with the Tri-Vac vaccine were intranasally challenged with 1×10^6 plaque-forming units (PFU) of live XBB.1.16 Omicron viruses and the animals were monitored for weight loss and changes in viral loads in throat swabs. On one day post-infection (dpi), the mice in the adjuvant group exhibited rapid weight loss, reaching

Fig. 5 | Tri-Vac is able to serve as a heterologous booster shot after vaccination of inactivated and mRNA vaccines. a–c NIH mice were intramuscularly immunized with three doses of prototypic SARS-CoV-2 inactivated vaccine (50U) followed by one dose of heterologous injection of Tri-Vac (IV×3 > Tri-Vac). The mice homologous vaccinated with four doses of inactivated virus vaccine (IV×3 > IV) were used as control (*n* = 5 mice per group). The schematic in (**a**) was created in BioRender. Wang, Y. (2024) BioRender.com/a77d348. The sera neutralizing antibodies against authentic viruses (**b**) and pseudoviruses (**c**) were determined. **d–f** NIH mice were intramuscularly immunized with three doses of 5 μg of mRNA/50 μl of encapsulated liposome (LPX)/Spike-mRNA followed by one dose of heterologous injection of Tri-Vac (mRNA×3 > Tri-Vac). The mice homologous vaccinated with four doses of mRNA vaccine (mRNA×3 > mRNA) were used as control (*n* = 5 mice per group). The schematic in (**d**) was created in BioRender. Wang, Y. (2024) BioRender.com/a77d348. The sera neutralization against authentic viruses

(**e**) and pseudoviruses (**f**) were determined. **g** The frequencies of Tfh and GC B cells in spleen tissues from mice in the group of homologous mRNA vaccination (mRNA×3 > mRNA) or heterologous Tri-Vac vaccination (mRNA×3 > Tri-Vac). **h** The frequencies of Tfh, GC B, and RBD-specific GC B cells in inguinal lymph nodes in groups of homologous or heterologous vaccination. The percentages of spike-specific CD4^{+} (**i**) and CD8^{+} (**j**) memory T cells in spleen tissues from mice immunized with four doses of mRNA vaccine or three doses of mRNA vaccine followed by Tri-Vac vaccination. Sera, spleen, and lymph node tissues were collected on day 14 after the final immunization. *n* = 5 mice per group in (**g, j**). Data are presented as geometric mean values with 95% CI in (**b, c, e, f**) and are presented as mean values with SEM in (**g, j**). *P*-values in (**b, c, e, f**) were determined by Two-way ANOVA analysis followed by Sidak's multiple comparisons test after the Log10 transformation, and in (**g, j**) were conducted by One-way ANOVA analysis followed by Tukey's multiple comparisons test. ns, not significant.
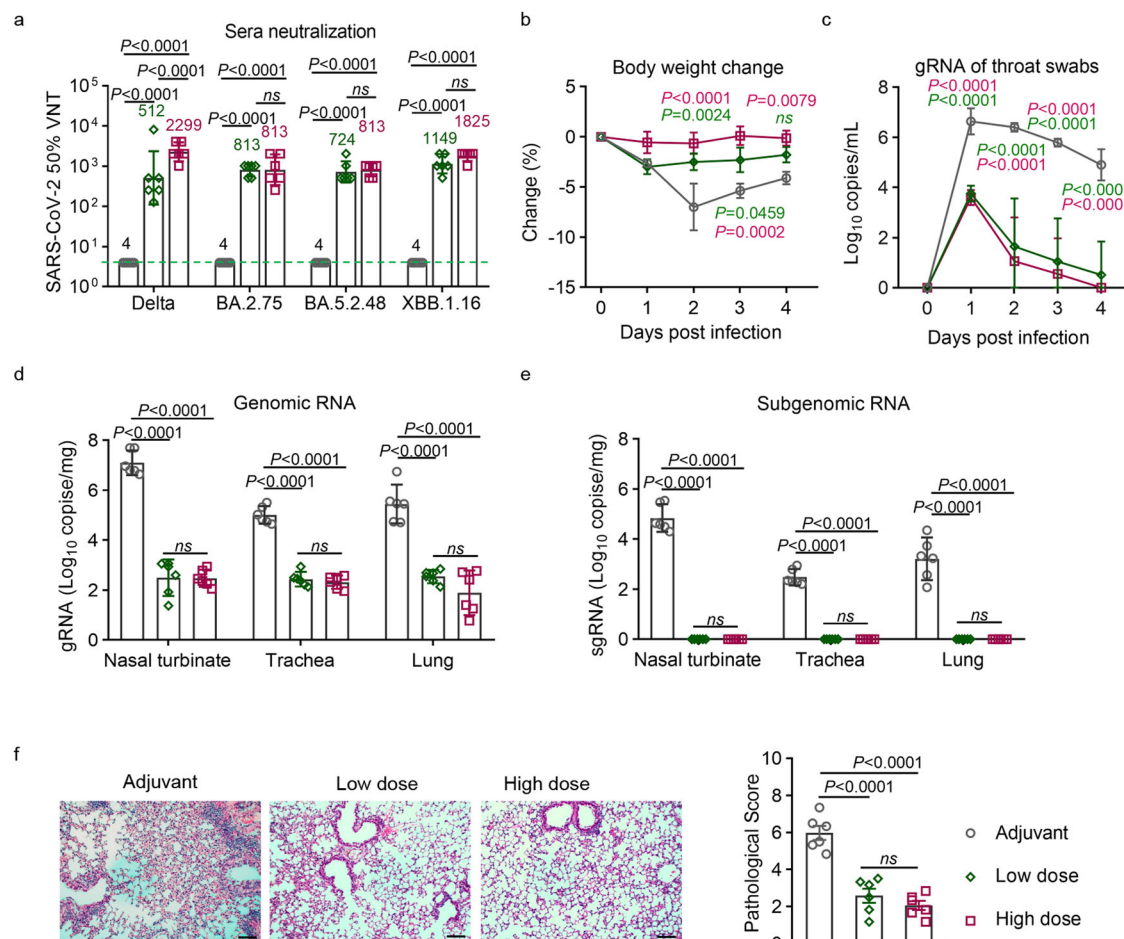

Fig. 6 | Tri-Vac provides protection against the infection of live Omicron XBB.1.16 virus. a NIH mice were immunized with three doses of 5 μg (low dose) or 10 μg (high dose) of Tri-Vac, and the sera neutralizing antibody titers against authentic SARS-CoV-2 viruses were determined. **b, c** NIH mice immunized with Tri-Vac were then challenged with 1 × 10⁶ PFU of live Omicron XBB.1.16 viruses via intranasal routes. Changes in body weight (**b**) and viral loads in throat swabs (**c**) post-SARS-CoV-2 infection were determined. **d, e** The infected mice were euthanized on day 4 post-infection, and multiple respiratory tissues, including nasal turbinates, trachea, and lung tissues, were collected to detect the levels of gRNA (**d**) and sgRNA (**e**) by RT-qPCR. **f** The histopathological changes and pathological

scores in the lung tissue from mice challenged with live XBB.1.16 virus. Scale bars represent 100 μm in (**f**). *n* = 6 mice per group in (**a–f**). Data are presented as geometric mean values with 95% CI in (**a, c–e**) and as mean with SEM in (**b, f**). *P* values in (**a, d, e**) were performed by Two-way ANOVA analysis followed by Tukey's multiple comparisons test after the Log10 transformation, in (**b**) were conducted by Two-way ANOVA analysis followed by Dunnett's multiple comparisons test (the group of Adjuvant was used as control), and in (**c**) were conducted by Two-way ANOVA analysis followed by Dunnett's multiple comparisons test after the Log10 transformation, and in (**f**) were performed by One-way ANOVA analysis followed by Tukey's multiple comparisons test. ns, not significant.

maximum weight loss on two dpi. In contrast, mice in the low-dose vaccine group showed slight and transient weight loss but rapidly rebounded, while those in the high-dose group showed no significant weight change throughout (Fig. 6b). In addition, high levels of viral genomic RNA (gRNA) were detected in throat swab samples from mice

in the adjuvant control group throughout the course of experimentation. However, immunization with low and high doses of Tri-Vac vaccine significantly reduced the viral loads in throat swabs (Fig. 6c). On day four dpi, the mice were euthanized for tissue processing to assay viral loads. As expected, both the low and high doses of the Tri-

Vac vaccine provided significant reductions in viral burden in multiple tissues of the respiratory system, including the nasal turbinate, trachea, and lung tissues (Fig. 6d). We also tested the sub-genomic RNA (sgRNA) in the tissues, which is an indicator of the active viral replication. sgRNA could be detected in all respiratory system tissues in the adjuvant group. In contrast, the sgRNA could not be detected in any tissues after immunization with the Tri-Vac vaccine (Fig. 6e). In addition, we observed that there was no statistical difference in levels of gRNA in throat swabs, and gRNA and sgRNA in respiratory system tissues between the low- and high-dose group. These results indicate that Tri-Vac can reduce viral loads and prevent the replication of live Omicron viruses in upper and lower respiratory tracts.

The effective protection by the Tri-Vac vaccine was also associated with significantly reduced histopathological changes. Mild pathologic changes, such as multifocal areas of consolidation, mild alveolar septa thickening, alveolar congestion, and small patches of inflammation composed of lymphocytes, neutrophils, and macrophage, could be observed in lung tissue from mice treated with adjuvant (Fig. 6f). In contrast, lung tissues collected from mice immunized with Tri-Vac showed a normal histological structure with intact pulmonary alveoli structure and with no apparent inflammation. The pathologic scores in the lung were significantly reduced in both low- and high-dose groups. Therefore, immunization with Tri-Vac can confer effective protection against live virus challenges in the upper and lower respiratory tracts.

Immunization with Tri-Vac improved neutralizing capacities in human participants

We subsequently initiated a phase 1 clinical investigator-initiated trial (IIT) to assess the safety and immunogenicity of Tri-Vac in human participants (Registration number: ChiCTR2200067245). The trial was conducted in strict adherence to the Ethics Committee Institution's principles. Eligible participants were required to meet specific inclusion and exclusion criteria, detailed in the Methods and clinical trial protocol. Participants were adults aged 18 years or older with a documented history of two or three doses of a COVID-19 vaccine administered over three months prior to the study. Participants were instructed to self-monitor and perform a SARS-CoV-2 antigen test prior to vaccination; those testing positive or presenting with an axillary temperature exceeding 37.3 °C were excluded to ensure that observed increases in neutralizing antibody responses were not attributed to recent natural infection. All participants understood the research procedures and were provided written informed consent. Informed consent was obtained from all participants, and a total of 64 adults were enrolled, with demographic characteristics and vaccination and infection histories detailed in Table 1 and Supplementary Table 1. Among the adult participants (aged from 22 to 67), 21 participants had received two doses of COVID-19 vaccine ($n = 11$ in low-dose, and $n = 10$ participants in high-dose group), 43 had received three doses of vaccines ($n = 21$ in low-dose, and $n = 22$ participants in high-dose group). The average interval between the last vaccination and this vaccination was 15.2 months. All participants had no SARS-CoV-2 infection history, and the results of the SARS-CoV-2 antigen test showed all participants were antigen-negative before vaccination.

The primary objective was to evaluate the tolerability and safety of Tri-Vac. Initially, five participants were enrolled in the low-dose group as sentinels and received a 30 μg injection of Tri-Vac. Upon completion of safety observations, an additional five participants were enrolled in the high-dose group and administered a 60 μg dose. Preliminary safety assessments indicated that both dosages were well-tolerated, with no serious adverse events. Consequently, enrollment in both groups continued with a 1:1 ratio, resulting in 32 participants per group receiving either the low or high dose of Tri-Vac (Fig. 7a).

The preliminary safety evaluations revealed that Tri-Vac was well-tolerated in both low- and high-dose recipients (Table 2). Within seven

Table 1 | Demographic and baseline characteristics

	Low dose group (N = 32)	High dose group (N = 32)	Total (N = 64)
Age			
Average age	35.5 (±13.0)	31.4 (±11.1)	33.5 (±12.2)
18–59 years n (%)	31 (96.88%)	31 (96.88%)	62 (96.88%)
≥60 years n (%)	1 (3.13%)	1 (3.13%)	2 (3.13%)
Gender			
Male n (%)	8 (25.00%)	3 (9.38%)	11 (17.19%)
Female n (%)	24 (75.00%)	29 (90.63%)	53 (82.81%)
Number of previous COVID-19 vaccinations			
Two dose n (%)	11 (34.38%)	10 (31.25%)	21 (32.81%)
Three dose n (%)	21 (65.63%)	22 (68.75%)	43 (67.19%)
Average vaccination interval			
Months	15.0 (9.2–20.5)	15.3 (9.3–20.7)	15.2 (9.2–20.7)

days post-injection solicited adverse events were reported by 8 participants (25.00%) in the high-dose group and 6 (18.75%) in the low-dose group. All reactions were mild, transient, and self-limiting, with no grade 3 reactions or serious adverse events. In the high-dose group, the most common adverse event was injection site pain (21.88%), followed by local redness (6.25%), swelling (6.25%), and induration (3.13%), and systemic fatigue (3.13%). In the low-dose group, local pain (12.50%) and systemic fever (3.13%) and headache (3.13%) were reported. Unsolicited adverse events within 30 days post-injection were reported by 9.38% of participants in both groups. In addition, no serious adverse events (SAEs) were reported within 6 months following vaccination in these participants.

To assess the immunogenicity of Tri-Vac, blood samples were collected pre-vaccination and on day 14 for neutralization assays. Pre-vaccination serum samples showed significantly impaired neutralization against Omicron variants, particularly the XBB lineage. However, a single dose of Tri-Vac substantially increased neutralizing antibody levels against all tested SARS-CoV-2 pseudoviruses, including pre-Omicron VOCs (prototype, Delta), BA.5, BF.7, BQ.1.1, and XBB lineages (XBB.1.5, XBB.1.9.1, XBB.1.16, XBB.2.3, EG.5.1, and HV.1) (Fig. 7b). To be specific, the GMTs in high dose group against prototype, Delta, BA.5, BF.7, BQ.1.1, XBB.1.5, XBB.1.9.1, XBB.1.16, XBB.2.3, EG.5.1 and HV.1 variants were increased by 3.0-, 4.2-, 6.8-, 8.3-, 4.1-, 16.3-, 11.3-, 4.7-, 9.0-, 10.8-, and 32.9-fold, respectively, and reached 1166, 1377, 1445, 2107, 1160, 911, 520, 533, 792, 507 and 1120, respectively. In low-dose group, the GMTs of neutralizing antibodies against these pseudoviruses were increased by 3.5-, 9.4-, 16.2-, 14.5-, 11.6-, 37.7-, 12.6-, 8.9-, 12.2-, 20.5- and 48.1-fold, respectively, and reached 1042, 1336, 3071, 1976, 1277, 1622, 593, 1092, 1063, 718, and 1154, respectively (Fig. 7b).

A recently emerged variant JN.1, an offshoot of the BA.2.86 with just one additional mutation (L455S) in RBD, has become predominant worldwide and accounts for 96.4% of currently circulating strains in the US[13,14]. Thus, we next assayed the neutralization against these subvariants after vaccination with Tri-Vac. We noticed the remarkable immune escape ability of JN.1 variants, while the Tri-Vac vaccination rescued the neutralizing capacities. Compared to pre-immunization, the GMTs of neutralizing antibodies in the group receiving high-dose of Tri-Vac to BA.2.86 and JN.1 variants were improved by 9.3- and 10.4-fold, respectively, and reached 1224 and 969. In addition, in the group receiving the low dose of vaccine, the GMTs to these variants were enhanced by 11.8- and 11.1-fold and were determined to be 1227 and 1001, respectively.

We then randomly selected fifteen serum samples from the low-dose group to perform an authentic virus neutralization assay, and the
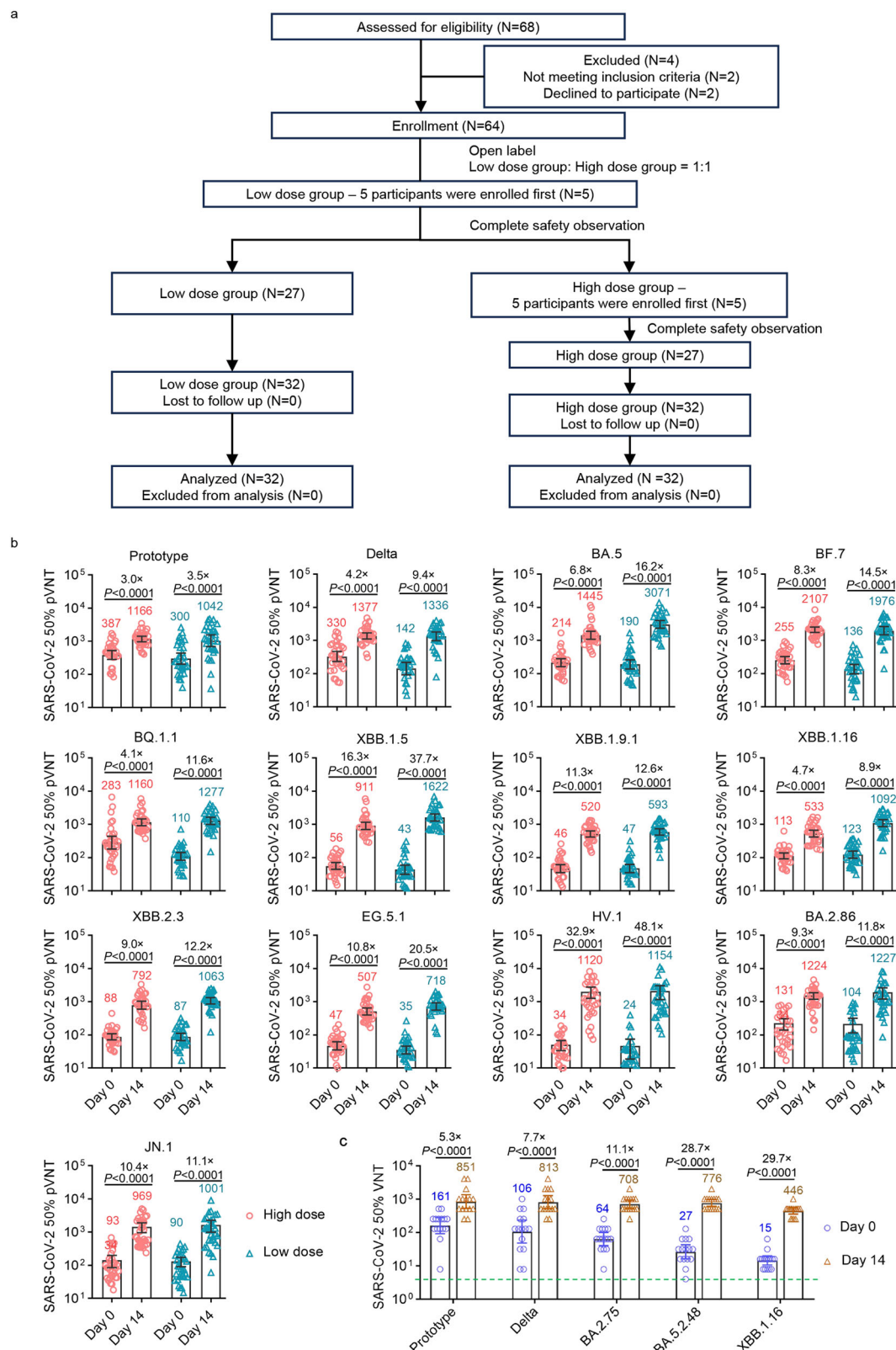
Fig. 7 | Tri-Vac improves neutralization capacities in human participants. a Flow diagram of enrollment of participants into the clinical investigator-initiated trial (IIT): 64 participants were recruited to evaluate the immunogenicity of the Tri-Vac vaccine. The human participants were assigned into two groups and received low-dose (green, 30 μg, $n = 32$) or high-dose (red, 60 μg, $n = 32$) of Tri-Vac. **b** The blood samples were collected and the neutralizing antibody titers in sera against prototype, Delta, BA.5, BF.7, BQ.1.1, XBB.1.5, XBB.1.9.1, XBB.1.16, XBB.2.3, EG.5.1, HV.1, BA.2.86 and JN.1 pseudoviruses were determined ($n = 32$ participants in high-dose group, and $n = 32$ participants in low-dose group). **c** Neutralizing antibodies in the low-dose group against authentic ancestral, Delta, BA.2.75, BA.5.2.48, and XBB.1.16 were determined ($n = 15$). Data are presented as geometric mean values with 95% CI. P values in (**b**, **c**) were conducted by Two-way ANOVA analysis followed by Sidak's multiple comparisons test multiple comparisons test after the Log10 transformation.

Table 2 | Summary of adverse events after vaccination

Adverse events	Low dose group (N = 32)		High dose group (N = 32)		Total (N = 64)	
	n	%	n	%	n	%
Solicited adverse events from Day 0–7	6	18.75	8	25.00	14	21.88
Local solicited adverse events	4	12.50	7	21.88	11	17.19
Vaccination site pain	4	12.50	7	21.88	11	17.19
Vaccination site swelling	0	0	2	6.25	2	3.13
Vaccination site redness	0	0	2	6.25	2	3.13
Vaccination site induration	0	0	1	3.13	1	1.56
Systemic solicited adverse events	2	6.25	1	3.13	3	4.68
Fever	1	3.13	0	0	1	1.56
Headache	1	3.13	0	0	1	1.56
Fatigue/Asthenia	0	0	1	3.13	1	1.56
Unsolicited adverse events from Day 0–30	3	9.38	3	9.38	6	9.38

results showed similar significant improvements in sera-neutralizing antibodies after boosting with a low-dose Tri-Vac vaccine. Compared to the levels of neutralizing antibody in sera collected pre-immunization, the GMTs of 50% neutralization in sera collected on day 14 after immunization against authentic ancestral, Delta, BA.2.75, BA.5.2.48 and XBB.1.16 were determined to 851, 813, 708, 776 and 446, and improved by 5.3-, 7.7-, 11.1-, 28.7-, and 29.7-fold, respectively, compared to that in sera collected pre-immunization (Fig. 7c). Long-term assessments of safety and immunogenicity for Tri-Vac were also conducted (Supplementary Fig. 4). No solid or unsolid adverse reactions were reported among participants six months post-vaccination. Additionally, pseudovirus neutralization assays showed that neutralizing activity was maintained for over six months in both the low- and high-dose groups, with serum-neutralizing antibody GMTs against the XBB.1.5 and JN.1 variants exceeding 800 and 600, respectively. These results demonstrated acceptable tolerability and good immunogenicity profile of Tri-Vac vaccine in human participants to improve cross-neutralization response.

Discussion

The SARS-CoV-2 pandemic persists, with the emergence of various subvariants such as Beta, Delta, Omicron BA.1, BA.2.75, BA.5, and BQ.1.1. Notably, the Omicron XBB lineage, including subvariants XBB.1.5, XBB.1.16, XBB.1.9.1, and subsequent strains EG.5.1, FL.1.5.1, and HV.1, have become globally dominant, leading to an increase in breakthrough infections. In addition to the XBB lineage, the Omicron branch represented by BA.2.86 and its descendant JN.1 have risen to prominence. The unpredictable evolution of the virus highlights the urgent need for next-generation, universal COVID-19 vaccines capable of inducing cross-neutralization against a range of variants. Our study presents a trivalent vaccine, Tri-Vac, combining HR-fused RBD trimeric proteins from Delta, BA.5, and XBB.1.5 variants at a 1:1:4 antigenic ratio. Tri-Vac induced robust and sustained humoral and cellular immune responses in mice, offering effective protection against respiratory tract infections from the live XBB.1.16 variant and serving as a promising candidate for booster shots to enhance cross-neutralization following initial vaccinations with inactivated or mRNA vaccines.

The global prevalence of XBB-lineages, characterized by significant evasion of prior vaccinations, has prompted Moderna and Pfizer/BioNTech to receive marketing authorization for a monovalent XBB.1.5 spike mRNA vaccine[20], and Novavax to develop an adjuvanted XBB.1.5 spike protein vaccine[21,22]. We also reported that the recombinant spike-XBB.1.5 antigen can induce a neutralization response against multiple Omicron subvariants[28]. Nevertheless, as shown in

Fig. 2c–f, antigen specifically matching to the XBB-lineage subvariants jeopardizes neutralization responses against several pre-Omicron VOCs due to the distinct antigenicity between Omicron variants to pre-Omicron VOCs[29,30]. Considering the unpredictable evolution of SARS-CoV-2, and future variants may not originate from the XBB lineage, we, therefore, successfully developed a universal vaccine with improved cross-neutralization responses against a variety of SARS-CoV-2 variants by incorporating antigens from both Omicron variants (BA.5 and XBB.1.5 subvariants) and pre-Omicron VOCs (Delta variant). Compared to the individual variant-specific antigen, we noticed that Tri-Vac induced broad-spectrum neutralizing antibodies, as evidenced by the regular polygonal representation on the radar map and the highest total 50% neutralizing antibody titers in mice from the group that received Tri-Vac. In addition, we have investigated the effects of different proportions of antigens (1:1:4, 1:2:3, 1:1:1) on neutralization, selecting the 1:1:4 ratio for Tri-Vac based on its high efficacy against Omicron XBB.1.5-included SARS-CoV-2 variants.

COVID-19 vaccines based on inactivated virus and mRNA platforms have demonstrated high efficacy in preventing symptomatic and severe disease[42,49,50]. mRNA vaccines have been rapidly updated to address emerging variants, evolving from the initial strain to bivalent vaccines containing wildtype and BA.4/5 spike proteins[2,51,52]. However, the neutralizing antibody response conferred by these vaccines faces challenges with the XBB lineages[2,15–17]. Consequently, Moderna and Pfizer/BioNTech updated their mRNA vaccine sequences to include the XBB.1.5 spike protein[20], with the XBB.1.5 monovalent mRNA vaccine booster showing strong neutralization against XBB and JN.1 subvariants[23]. Despite the marketing authorization of monovalent XBB.1.5 mRNA vaccine by Moderna and Pfizer/BioNTech, considering the widespread global administration of mRNA-based COVID-19 vaccines, opting for heterologous vaccination with an alternative vaccine platform such as subunit protein may provide additional advantages in improving immune response than repeated homologous vaccination with mRNA-based vaccines[46–48]. In this study, heterologous boosting with Tri-Vac after three doses of inactivated or mRNA vaccine based on the antigen from pre-XBB lineages significantly rescued the sera levels of neutralizing antibodies against multiple SARS-CoV-2 in mice. In addition, strong germinal center and antigen-specific T cell responses were induced by heterologous injection of Tri-Vac after three doses of mRNA vaccine, indicating its potential for a heterologous vaccination program. A previous study reported heterologous second immunization of mRNA-1273 (Moderna), but not a protein-adjuvant vaccine (NVX-CoV2373, Novavax), provided increases in antibody response after prime mRNA vaccine (BNT162b2, Pfizer/BioNTech) compared with homologous schedules in humans[53]. Nevertheless, given the differences in vaccine antigen components, doses of previous vaccinations, and hybrid immune backgrounds in the population, the effectiveness of boosting with Tri-Vac in humans should be further investigated in future clinical trials.

In addition to the pre-clinical study, we also conducted an IIT to evaluate the transition of vaccines into clinical use for human protection. The preliminary results in IIT showed good safety and immunogenicity of Tri-Vac as an extra booster shot in 64 adult participants who had previously received two or three doses of the COVID-19 vaccine. Both low and high doses of Tri-Vac provide significant improvements in neutralizing antibodies against multiple SARS-CoV-2 variants. Even for the recently circulating JN.1 variant that originated from BA.2.86 and has significantly distinct spike mutations compared with BA.2 and XBB.1.5, the GMTs of neutralization against this variant in a group of low- and high-dose Tri-Vac were improved by 10.4- and 11.1-fold, respectively, compared to pre-immunization sera. It is noteworthy that the improvements in neutralizing antibodies induced by the low-dose Tri-Vac are comparable to those in the high-dose group, potentially due to participants' pre-existing immunity from prior vaccinations. Given these results and the lower incidence of adverse reactions in the

low-dose group, we have decided to use a dose of 30 μg of antigen protein with adjuvant for emergency use vaccination in China, consistent with the low dose used in the clinical study.

Despite these promising findings, the small sample size of only 64 participants limits the conclusions that can be drawn; thus, these data should be considered preliminary regarding the safety and immunogenicity of Tri-Vac. Due to the limited number of enrolled individuals, we were unable to conduct stratified analyses of safety and immunogenicity by age, gender, or underlying conditions. Additionally, while cellular immunity is crucial for long-term protection against viruses, we regret that we did not collect data on cellular immunity, such as assessing IFN-γ secretion from PBMCs over an extended period (3 or 6 months) after the booster. We planned to evaluate the safety and immunogenicity of Tri-Vac vaccine in a phase 2 clinical trial and aimed to evaluate the efficacy against COVID-19 in a randomized, double-blind, placebo-controlled Phase 3 clinical trial. The vaccine efficacy would be measured by calculating the relative risk of getting symptomatic virologically confirmed COVID-19 in the vaccinated group versus the placebo group. Approved for emergency use in China by the Chinese Center for Disease Control and Prevention (CDC, https://www.chinacdc.cn/jkzt/crb/zl/szkb_11803/jszl_11815/202308/t20230801_268283.html), Tri-Vac's performance will be closely monitored. This study represents an approach to universal COVID-19 vaccine design, integrating antigens from diverse SARS-CoV-2 strains to address the ongoing pandemic.

Methods

Ethics statement
All mice vaccination experiments have been approved by the Institutional Animal Care and Use Committee of Sichuan University (ethical approval No. 20220531062).

All procedures related to the animals challenged with the live SARS-CoV-2 XBB.1.16 viruses were reviewed and approved by the Institutional Animal Care and Use Committee of the Institute of Medical Biology, Chinese Academy of Medical Sciences, and performed in the ABSL-4 facility of Kunming National High-level Biosafety Primate Research Center (ethical approval No. DWSP202206).

All operations and procedures involving human participants in the phase 1 clinical investigator-initiated trial (IIT) were reviewed and approved by the Ethics Committee of West China Hospital (Registration number: ChiCTR2200067245).

Cells and viruses
Sf9 insect cells (CRL-1711) were obtained from the American Type Culture Collection (ATCC) and maintained in SIM SF medium (Sino Biological, Cat: MSF1) at a non-humidified shaker at 28 °C. Vero E6 cells were kindly provided by the Chinese Academy of Medical Sciences and Peking Union Medical College, and ACE2-expressing HEK293T cells (293T/ACE2) were constructed by our group. Vero E6 and 293T/ACE2 cells were cultured in DMEM medium (Gibco, Cat: REFC11995500BT) containing 10% fetal bovine serum (PAN Biotech, Cat: ST30-3302). SARS-CoV-2 pseudoviruses, including the prototype (Cat: GM-21318LV), Delta (Cat: GM-32040LV), BA.2.75 (Cat: GM-53320LV), BA.5 (Cat: GM-51543LV), BF.7 (Cat: GM-55890LV), BQ.1 (Cat: GM-57378LV), BQ.1.1 (Cat: GM-59399LV), XBB (Cat: GM-56686LV), XBB.1.5 (Cat: GM-59400LV), XBB.1.6 (Cat: GM-75235LV), XBB.1.9.1 (Cat: GM-75040LV), XBB.1.16 (Cat: GM-76228LV), XBB.2.3 (Cat: GM-75188LV), EG.5.1 (Cat: GM-80273LV), HV.1 (Cat: GM-82129LV), BA.2.86 (Cat: GM-80181LV) and JN.1 (Cat: GM-84672LV), were provided by Genomeditech. Live SARS-CoV-2 strains (Delta, BA.2.75, BA.5.2.48, and XBB.1.16 strains) were cultured and tested in the biosafety level 3 (P3) facilities in accordance with the relevant guidelines at the National Kunming High-level Biosafety Primate Research Center.

The preparation of trimeric RBD-HR proteins
The design that uses the self-assembled feature of the HR sequence to express trimeric RBD-HR proteins has been described in our previous study[31]. In the current study, the sequence of RBD (320-545 aa) derived from the SARS-CoV-2 BA.5 or XBB.1.5 variant was directly linked in tandem with HR1 (916-966 aa) and HR2 (1157-1203 aa) in S2 subunit of the spike protein. In addition, the C538 residue was substituted with a serine residue (C538S) as C538 residue in RBD might form an inter-chain disulfide bond and subsequently lead to dimerization of the RBD subunit to cause irregular protein aggregation. The designed protein sequence was fused with the sequences of a GP67 signal peptide for protein secretion and a Trx tag for protein folding at its N-terminal in a tandem manner. In addition, a 6×His tag was added to facilitate initial affinity-chromatographic purification of the protein from the insect cell culture, and an enterokinase (EK) cleavage site was designed for tag removal.

The $RBD_{BA.5}$-HR and $RBD_{XBB.1.5}$-HR proteins were expressed using the classic Bac-to-Bac Baculovirus Expression System (Invitrogen)[31,54]. Briefly, the gene described above was amplified and incorporated into the pFastBac1 vector. Then, the validated plasmid was transformed into *Escherichia coli* DH10b cells to produce recombinant bacmids. Next, we transferred recombinant bacmids into Sf9 insect cells to express protein antigens. Finally, the proteins were cleaved by the EK protease, purified by Superdex 200 Increase 10/300 GL column, and determined by Coomassie blue staining and Western blotting (Rabbit anti-SARS-CoV-2 Spike antibody, 40150-R007, Sino Biological). In order to identify the successful cleavage of the Trx-His-EK tag by enterokinase, Coomassie staining and N-terminal sequencing using the Edman degradation method[55] were performed. The proteins were transferred to the PVDF membrane, excised, and sequenced using a PPSQ 53A sequencer with PTH as standard. In addition, negative-staining transmission electron microscopy (TEM) was further performed to determine the structure of trimeric $RBD_{BA.5}$-HR and $RBD_{XBB.1.5}$-HR proteins.

Generation of the RBD-HR trimer model using PyMOL
The model of the RBD-HR trimer was generated using PyMOL (version 2.6, http://pymol.sourceforge.net). The RBD structure was derived from PDB code 7wbp, and the helical HR-bundle structure was derived from PDB code 6lxt. To generate the model, three RBDs were moved in PyMOL to the top of the HR bundle and finely adjusted to give an overall bouquet-like structure. The image of the model was then generated by coloring the three RBDs and the HR bundle in green, cyan, magenta, and yellow, respectively.

Vaccine preparation
For the preparation of Tri-Vac with an antigenic ratio of 1:1:4, a total of 10 μg recombinant proteins that contained RBD_{Delta}-HR, $RBD_{BA.5}$-HR, and $RBD_{XBB.1.5}$-HR proteins were dissolved in 50 μl PBS solution and then mixed with MF59-like oil-in-water adjuvant at a 1:1 volume ratio to the final volume of 100 μl. In addition, the adjuvant-formulated RBD_{Delta}-HR (1.67 μg, 10 μg), $RBD_{BA.5}$-HR (1.67 μg, 10 μg) or $RBD_{XBB.1.5}$-HR (6.67 μg, 10 μg) proteins, and trivalent vaccines with antigenic ratio of 1:1:1 or 1:2:3 were also prepared as described above.

Vaccination of mice
Specific pathogen-free (SPF) female NIH mice (6–8 weeks) were provided by Beijing Vital River Laboratory Animal Technologies Co., Ltd (China) and maintained in an SPF animal facility (temperature: 21–25 °C; humidity: 30–70 %; dark/light cycle: 12 h/12 h) in the animal center of the State Key Laboratory of Biotherapy. Only female mice were chosen for animal experiments because sex was not considered as a biological variable in this study. All mice were adapted for one week and then grouped randomly. All mice experiments have been approved by the Institutional Animal Care and Use Committee of Sichuan University (ethical approval No. 20220531062).

NIH mice were intramuscularly immunized with Tri-Vac and adjuvant-formulated antigen proteins as indicated in each figure and figure legend following the same prime-boost regimen spaced 21 days apart (immunization on days 0, 21, and 42). The mice were bled to death under deep anesthesia and the sera and tissue samples were collected on day 56.

For the heterologous booster immunization, female NIH mice were first intramuscularly vaccinated with three doses of 50U of prototypic SARS-CoV-2 inactivated vaccine VacKMS1 that was developed by Medical Biology (IMB), Chinese Academy of Medical Sciences (CAMS)[50], or with three doses of mRNA vaccine (5 μg per mouse) developed by us that based on the sequence of SARS-CoV-2 Delta full-length spike protein (mRNA)[56] at weeks 0, 2 and 6. At week 16, one group of mice was immunized with one dose of Tri-Vac after injections of inactivated vaccine (IV×3 > Tri-Vac) or mRNA vaccine (mRNA×3 > Tri-Vac). The mice vaccinated with four doses of inactivated vaccine (IV×3 > IV) or mRNA vaccine (mRNA×3 > mRNA) were used as homologous immunization control. The sera and tissue samples were collected on day 14 after the final immunization.

Binding antibody measurement using enzyme-linked immunosorbent assay (ELISA)

To detect the antigen-specific IgG antibody in sera, 96-well plates (NUNC-MaxiSorp, Thermo Fisher Scientific) were coated with RBD_{Delta}-HR, $RBD_{BA.5}$-HR or $RBD_{XBB.1.5}$-HR proteins (1 μg/ml) in carbonate coating buffer at 4 °C for 12–16 h. Then, the 96-well plates were washed three times with PBST (PBS containing 0.1% Tween-20) and blocked with blocking buffer (PBST containing 1% BSA) for one h at 37 °C. Next, the plates were washed one time, and diluted sera samples were added to the wells (100 μl/well). The plates were then incubated for 1 h at 37 °C and washed by PBST three times. Horseradish peroxidase (HRP)-conjugated anti-mouse IgG antibodies (1:10,000, southern biotech, Cat: 0107-05) were added to the wells (100 μl/well) and incubated for one h at 37 °C. After washing five times, each plate was added to 3,3′,5,5′-tetramethyl biphenyl diamine (TMB, P0206, Biyotime) and developed for 10 min at room temperature. The reaction was stopped with 1 M H_2SO_4, and the absorbance was measured at 450 nm on a microplate reader (Spectramax ABS, Molecular Devices).

SARS-CoV-2 pseudovirus neutralization assays

The sera samples were inactivated at 56 °C for 30 min before three-fold diluted, and then incubated with diluted pseudoviruses at 37 °C for one h in 96-well plates (Cat: WHB-96-03, Shanghai Wohong Biotechnology Co., Ltd.). HEK-293T cells expressing human ACE2 receptor (293 T/ACE2) were collected and added to each well ($1.5 × 10^4$/well). The plates were incubated in a 37 °C incubator for 48 h. After removing the supernatant in plates, 50 μl PBS and 50 μl lysis reagent with luciferase substrate (Beyotime, RG005) were added to each well. The luminescence intensity was determined by a multi-mode microplate reader (PerkinElmer, USA), and the 50% neutralization titers were calculated by GraphPad Prism 8.0.2.

Live SARS-CoV-2 virus neutralization assays

Authentic SARS-CoV-2 viruses, including Delta, BA.2.75, BA.5.2.48, and XBB.1.16 strains, were used to detect the titers of neutralizing antibodies in immunized sera. In brief, Vero E6 cells ($5 × 10^4$/well) were seeded in microplates and incubated overnight to adherent. The inactivated sera were 2-fold diluted by DMEM complete medium and mixed with 50 μl live SARS-CoV-2 viruses (MOI = 0.01) to a final volume of 100 μl and incubated for 1 h at 37 °C, then added the mixtures to plates covered with cells and incubated for 72–96 h in a 37 °C incubator. Microscopy was used to detect the cytopathogenic effects (CPE), the Karber method was used to calculate the titer of neutralizing antibodies, and the NT50 (50% neutralization titer) is the reciprocal of the maximum serum dilution that causes 50% cell infection[50].

Enzyme-linked immunospot assay (ELISpot)

For the detection of antibody-secreting cells (ASCs) in spleen and bone marrow, sterile 96-well ELISpot filter plates (REF: MSIPS4W10, Millipore, USA) were treated with 30 μl 35% ethanol/well for 1 min and then washed four times with sterile water. The preprocessed plates were coated with 3 μg/ml of $RBD_{XBB.1.5}$-HR protein overnight at 4 °C, and then blocked with culture medium (1640 complete medium) for 2 h at 37 °C. Subsequently, isolated lymphocyte cells ($1 × 10^5$/well) from tissues were added to the plates and incubated at 37 °C overnight. The next day, the plates were washed with PBS 4 times and incubated with 100 μl/well HRP-conjugated goat anti-mouse IgG antibody (1:10000, Cat: 0107-05, Southern Biotech) for 2 h at room temperature. After washing with PBS 4 times, TMB ELISpot substrate solution (100 μl/well, Cat:3651-10, Mabtech, Sweden) was added to the plates until a distinct spot emerged. The reaction was stopped in running tap water. The plates were left to dry before capturing and counting spots with ELISpot Reader (CTL S6 Ultra M2, USA).

Flow cytometry

Lymphocytes from the spleen tissues were isolated under sterile conditions, seeded in 12-well plates ($1 × 10^6$/well), cultured with 1640 complete medium (10% FBS, 100 μg/ml streptomycin, 100 U/ml penicillin, 1 mM pyruvate, 50 μM β-mercaptoethanol, and 20 U/ml IL-2), and stimulated with three peptide pools (1 μg/ml,15mers with 11 aa overlap) covering spike protein of wildtype (Cat: RP30020, GenScript), BA.4/5 (Cat: RP30223CN, GenScript) and XBB.1.5 (Customer designed, GenScript) variant, respectively, for 12 h. The cells were then treated with a protein transport inhibitor (Cat: 555029, BD Biosciences) containing brefeldin A for 6 h before collecting for detection. The cells were stained with PerCP/Cyanine5.5-conjugated anti-mouse CD3 (Cat:100218), FITC-conjugated anti-mouse CD4 (Cat:100406), APC-conjugated anti-mouse CD8a (Cat:100712) and Brilliant Violet 510 anti-mouse/human CD44 (Cat:103044) at 4 °C for 30 min. After being washed with PBS three times, cells were fixed and permeabilized by the Fixation/Permeabilization Kit (Cat: 554715, BD Biosciences) at room temperature for 20 min. Then, perforated cells were stained with PE-conjugated anti-mouse IFN-γ (Cat:505808) and Brilliant Violet 421 anti-mouse TNF (Cat:506328) at room temperature for one h.

For the assay of GC B cells in spleen and inguinal lymph nodes, cells were stained with the following antibodies including PerCP/Cyanine5.5 anti-mouse CD3 (Cat:100218), Brilliant Violet 605 anti-mouse CD19 (Cat: 115540), PE/Cyanine7 anti-mouse CD95 (Cat:152618) and Pacific Blue anti-mouse/human GL7 (Cat: 144614). The antigen-specific GC B cells were detected by incubation with recombinant biotinylated $RBD_{XBB.1.5}$ proteins (SPD-C82Q3, ACRO) for 30 min before cell staining. For assay of percentages of Tfh cells in spleen and lymph nodes, Brilliant Violet 605 anti-mouse CD19, PerCP/Cyanine5.5 anti-mouse CD3, FITC anti-mouse CD4, Brilliant Violet 421 anti-mouse CXCR5 (Cat: 145512) and PE anti-mouse PD-1 antibodies (Cat: 114118) were used to stained.

The MBCs were detected with PerCP/Cyanine5.5 anti-mouse CD3, Brilliant Violet 605 anti-mouse CD19, FITC anti-mouse/human CD45R/B220 (Cat:103206), Brilliant Violet 510 anti-mouse IgD (Cat:405723), PE/Cyanine7 anti-mouse CD38 (Cat:165612) and Pacific Blue anti-mouse/human GL7 antibodies. In addition, the LLPCs were stained with FITC anti-mouse CD45 (Cat: 147710), Brilliant Violet 510 anti-mouse IgD, Brilliant Violet 650 anti-mouse CD138 (Cat: 142518) and PE/Cyanine7 anti-mouse/human CD45R/B220 (Cat: 103222) antibodies. All antibodies were purchased from BioLegend, detailed information was presented in Supplementary Table 2. Gating strategies of each immune cell were provided in Supplementary Fig. 3. Cells were detected and analyzed using the NovoCyte Advanteon Flow Cytometer with NovoExpress 1.5.6 (Agilent).

The challenge of mice with live SARS-CoV-2 XBB.1.16 Omicron variant

The female NIH mice (6-8 weeks) were intramuscularly immunized with (1) MF59-like adjuvant, (2) low-dose (5 µg), and (3) high-dose (10 µg) of Tri-Vac on days 0, 21, and 42. Then, the mice were intranasally challenged with 1×10^6 PFU live SARS-CoV-2 XBB.1.16 Omicron variant on day 63 since the first immunization. Body weight changes and viral loads in throat swabs were monitored daily. For the collection of throat swab samples, anesthetize the mice with 5% isoflurane, then insert a pre-soaked disposable swab containing PBS into the pharyngeal, gently wipe and slowly rotate the swab. After collecting the secretions sample, the swabs were immersed in a tube containing Trizol for subsequent viral load assay.

On day four post-infection, the mice were euthanized, and the tissues were collected to determine the viral loads and pathological changes. Viral genomic RNA (gRNA) and sub-genomic RNA (sgRNA) in nasal turbinate, trachea, and lung tissue samples were performed by a reverse-transcription quantitative polymerase chain reaction (RT-qPCR) assay, and the pathological changes in lung tissues were evaluated by hematoxylin and eosin staining (H&E).

The following primer and probe sequences (synthesized by Tsingke Biotech), including 5′-GACCCCAAAATCAGCGAAAT-3′ (forward), 5′-TCTGGTTACTGCCAGTTGAATCTG-3′ (reverse), 5′-FAM-ACNGCCGCATTACGTTTGGTGGACC-BHQ1-3′ (probe sequence) were used to detect gRNA in the RT-qPCR assay. SARS-CoV-2 sub-genomic RNA gene using the following primer and probe sequences: 5′-CGATCTCTTGTAGATCTGTTCTC-3′ (forward); 5′-ATATTGCAGCAG-TACGCACACA-3′ (reverse); 5′-FAM-CGAAGCGCAGTAA GGATGGC-TAGTGT-BHQ1-3′ (probe). All procedures related to the animals challenged with the live SARS-CoV-2 XBB.1.16 viruses were reviewed and approved by the Institutional Animal Care and Use Committee of the Institute of Medical Biology, Chinese Academy of Medical Sciences (ethical approval No. DWSP202206), and performed in the ABSL-4 facility of Kunming National High-level Biosafety Primate Research Center.

Study design of the evaluation of safety and immunogenicity of Tri-Vac in human participants

The phase 1 clinical investigator-initiated trial (IIT) was conducted to evaluate the safety and efficacy of the Tri-Vac vaccine in human participants (Registration number: ChiCTR2200067245, Date of registration: December 30, 2022, https://www.chictr.org.cn/showproj.html?proj=188473). The Ethics Committee of West China Hospital reviewed and approved the research involving humans. All participants recruited for this study should provide written informed consent and were required to meet the elaborate inclusion and exclusion criteria below:

1. Inclusion Criteria
1. 18 years of age and older;
2. Capable of giving personal signed informed consent;
3. Participants who are willing and able to comply with the requirements of this protocol and are able to comply with all scheduled visits;
4. Vaccinated with 2 or 3 doses of COVID-19 vaccine with a time interval of more than 3 months between the last dose and this vaccination;
5. Fertile men and women of childbearing potential voluntarily use effective contraceptive measures, including abstinence or effective contraceptive measures (such as intrauterine or implantable contraceptive devices, oral contraceptives, injectable or implanted contraceptives, sustained-release local contraceptives, intrauterine devices (IUDs), condoms (male), diaphragm, cervical cap, etc.) from the time of signing the informed form until 3 months after vaccination.
2. Exclusion Criteria

1. Positive SARS-CoV-2 antigen test at screening (conducted by a commercialized SARS-CoV-2 antigen detection kit (Company: YHLO, Cat: G86257));
2. Allergic to any component of the study vaccine, history of severe vaccine allergic reaction, allergy or asthma;
3. History or family history of convulsion, epilepsy, encephalopathy and psychosis;
4. Occurrence of vaccination-related serious adverse reactions after previous vaccination with COVID-19 vaccine;
5. Axillary body temperature ≥ 37.3 °C;
6. Patients with severe cardiovascular diseases, such as arrhythmia, conduction block, myocardial infarction, severe hypertension that cannot be controlled by drugs;
7. Suffering from severe chronic diseases or the disease is in the progressive stage which cannot be controlled smoothly, such as diabetes and thyroid disease;
8. Congenital or acquired angioedema/neuroedema;
9. Urticaria 1 year before receiving the study vaccine;
10. Asplenia or functional asplenia;
11. Women who are pregnant or breastfeeding, or plan to become pregnant or donate eggs during the study;
12. Any medical, psychological, social or other condition that, in the judgment of the investigator, violates the trial protocol.

In this IIT, we recruited 64 adult participants 18 years and older with a history of two or three doses of COVID-19 vaccines with an interval of more than three months after the last vaccination and who were not infected during vaccination. Five participants were enrolled as sentinel participants and received one injection of 30 µg of Tri-Vac (Good Manufacturing Practice, GMP, WestVac Biopharma Co., Ltd.) in the lateral deltoid muscle of the upper arm for safety evaluation. After the completion of safety observations of these persons, another 5 participants were recruited into the high-dose group and administered with 60 µg of Tri-Vac. Then, the enrollment of remaining participants in the low- and high-dose groups was simultaneously initiated, and participants were assigned to these two groups with a 1:1 ratio of numbers. Finally, 32 participants were recruited to the low-dose group and 32 persons to the high-dose group. This deviates from the sample size ($n = 100$ participants) specified in the protocol because the analysis of the 64 recruited participants provides sufficient confidence to achieve the trial objectives for evaluating the safety and immunogenicity of the Tri-Vac vaccine in human participants. Therefore, we terminated this clinical trial, which was also in accordance with IIT clinical trial ethics.

All participants were requested to complete an online diary to record any adverse reactions within seven days of vaccination. The blood samples were collected before vaccination and collected on indicated days (7, 14, 30 days, and 3, 6 months) after immunization, and the sera were stored at −80 °C for subsequent neutralization antibody assays. Given the representative nature of serum samples collected on day 14 post-immunization for assessing neutralizing antibody levels, these data have been included in the current study. Participation in this study was completely voluntary, and no transportation or nutritional compensation would be provided. During this study, participants would be entitled to free treatment for any study-related injury that was determined to be directly related to this study and compensation for any serious adverse event that was determined to be directly related to this study.

Statistics and reproducibility

All experiments except the SARS-CoV-2 challenge experiment in animals and in the clinical trial were repeated independently at least twice with similar results. GraphPad Prism 8.0.2 software was used for statistical analysis. The data are presented as geometric mean values with 95% confidence intervals (CI) or mean values with SEM, as presented in

each figure legend. Significance values were calculated using one-way or two-way ANOVA, as presented in each figure legend. Two-tailed unpaired student's *t*-tests analyzed comparisons between two groups. *P* values of <0.05 were considered significant.

Reporting summary

Further information on research design is available in the Nature Portfolio Reporting Summary linked to this article.

Data availability

All data supporting findings in the study are available in the main text and supplementary information or from the corresponding author on request. Source data are provided with this paper.

References

1. Uraki, R. et al. Humoral immune evasion of the omicron subvariants BQ.1.1 and XBB. *Lancet Infect. Dis.* **23**, 30–32 (2023).
2. Kurhade, C. et al. Low neutralization of SARS-CoV-2 Omicron BA.2.75.2, BQ.1.1 and XBB.1 by parental mRNA vaccine or a BA.5 bivalent booster. *Nat. Med.* **29**, 344–347 (2023).
3. Viana, R. et al. Rapid epidemic expansion of the SARS-CoV-2 Omicron variant in southern Africa. *Nature* **603**, 679–686 (2022).
4. Yamasoba, D. et al. Virological characteristics of the SARS-CoV-2 Omicron BA.2 spike. *Cell* **185**, 2103–2115.e2119 (2022).
5. Cao, Y. et al. BA.2.12.1, BA.4 and BA.5 escape antibodies elicited by Omicron infection. *Nature* **608**, 593–602 (2022).
6. Wang, Q. et al. Alarming antibody evasion properties of rising SARS-CoV-2 BQ and XBB subvariants. *Cell* **186**, 279–286.e278 (2023).
7. Uriu, K. et al. Enhanced transmissibility, infectivity, and immune resistance of the SARS-CoV-2 omicron XBB.1.5 variant. *Lancet Infect. Dis.* **23**, 280–281 (2023).
8. Qu, P. et al. Enhanced evasion of neutralizing antibody response by Omicron XBB.1.5, CH.1.1, and CA.3.1 variants. *Cell Rep.* **42**, 112443 (2023).
9. Faraone, J. N. et al. Immune evasion and membrane fusion of SARS-CoV-2 XBB subvariants EG.5.1 and XBB.2.3. *Emerg. Microbes Infect.* **12**, 2270069 (2023).
10. Kaku, Y. et al. Antiviral efficacy of the SARS-CoV-2 XBB breakthrough infection sera against omicron subvariants including EG.5. *Lancet Infect. Dis.* **23**, e395–e396 (2023).
11. Wang, Q. et al. Antibody neutralisation of emerging SARS-CoV-2 subvariants: EG.5.1 and XBC.1.6. *Lancet Infect. Dis.* **23**, e397–e398 (2023).
12. Ciccozzi, A. et al. The mutation point of view of the SARS-CoV-2 HV.1 lineage. *J. Med. Virol.* **96**, e29359 (2024).
13. CDC. CDC data tracker, <https://covid.cdc.gov/covid-data-tracker/#variant-proportions. > (2023).
14. Yang, S. et al. Fast evolution of SARS-CoV-2 BA.2.86 to JN.1 under heavy immune pressure. *Lancet Infect. Dis.* **24**, e70–e72 (2024).
15. Davis-Gardner, M. E. et al. Neutralization against BA.2.75.2, BQ.1.1, and XBB from mRNA Bivalent Booster. *N. Engl. J. Med.* **388**, 183–185 (2023).
16. Miller, J. et al. Substantial neutralization escape by SARS-CoV-2 Omicron variants BQ.1.1 and XBB.1. *N. Engl. J. Med.* **388**, 662–664 (2023).
17. Zou, J. et al. Neutralization of BA.4-BA.5, BA.4.6, BA.2.75.2, BQ.1.1, and XBB.1 with bivalent vaccine. *N. Engl. J. Med.* **388**, 854–857 (2023).
18. Uraki, R. et al. Antiviral and bivalent vaccine efficacy against an omicron XBB.1.5 isolate. *Lancet Infect. Dis.* **23**, 402–403 (2023).
19. Yang, J. et al. Low levels of neutralizing antibodies against XBB Omicron subvariants after BA.5 infection. *Signal Transduct. Target. Ther.* **8**, 252 (2023).
20. Huang, C. Q., Vishwanath, S., Carnell, G. W., Chan, A. C. Y. & Heeney, J. L. Immune imprinting and next-generation coronavirus vaccines. *Nat. Microbiol.* **8**, 1971–1985 (2023).
21. Lin, D. Y. et al. Durability of XBB.1.5 vaccines against Omicron subvariants. *N. Engl. J. Med.* **390**, 2124–2127 (2024).
22. Patel, N. et al. XBB.1.5 spike protein COVID-19 vaccine induces broadly neutralizing and cellular immune responses against EG.5.1 and emerging XBB variants. *Sci. Rep.* **13**, 19176 (2023).
23. Wang, Q. et al. XBB.1.5 monovalent mRNA vaccine booster elicits robust neutralizing antibodies against XBB subvariants and JN.1. *Cell Host Microbe* **32**, 315–321.e313 (2024).
24. Lustig, Y. et al. Humoral response superiority of the monovalent XBB.1.5 over the bivalent BA.1 and BA.5 mRNA COVID-19 vaccines. *Vaccine* **42**, 126010 (2024).
25. Stankov, M. V. et al. Humoral and cellular immune responses following BNT162b2 XBB.1.5 vaccination. *Lancet Infect. Dis.* **24**, e1–e3 (2024).
26. Yu, X. et al. Safety, immunogenicity, and preliminary efficacy of a randomized clinical trial of omicron XBB.1.5-containing bivalent mRNA vaccine. *hLife* **2**, 113–125 (2024).
27. Zhao, F., Zai, X., Zhang, Z., Xu, J. & Chen, W. Challenges and developments in universal vaccine design against SARS-CoV-2 variants. *NPJ vaccines* **7**, 167 (2022).
28. He, C. et al. A recombinant spike-XBB.1.5 protein vaccine induces broad-spectrum immune responses against XBB.1.5-included Omicron variants of SARS-CoV-2. *MedComm* **4**, e263 (2023).
29. Mykytyn, A. Z. et al. Antigenic cartography of SARS-CoV-2 reveals that Omicron BA.1 and BA.2 are antigenically distinct. *Sci. Immunol.* **7**, eabq4450 (2022).
30. Mykytyn, A. Z. et al. Antigenic mapping of emerging SARS-CoV-2 omicron variants BM.1.1.1, BQ.1.1, and XBB.1. *Lancet Microbe* **4**, e294–e295 (2023).
31. He, C. et al. A self-assembled trimeric protein vaccine induces protective immunity against Omicron variant. *Nat. Commun.* **13**, 5459 (2022).
32. Sun, H. et al. Structural basis of HCoV-19 fusion core and an effective inhibition peptide against virus entry. *Emerg. Microbes Infect.* **9**, 1238–1241 (2020).
33. Xia, S. et al. Inhibition of SARS-CoV-2 (previously 2019-nCoV) infection by a highly potent pan-coronavirus fusion inhibitor targeting its spike protein that harbors a high capacity to mediate membrane fusion. *Cell Res.* **30**, 343–355 (2020).
34. Peng, Y. et al. Broad and strong memory CD4(+) and CD8(+) T cells induced by SARS-CoV-2 in UK convalescent individuals following COVID-19. *Nat. Immunol.* **21**, 1336–1345 (2020).
35. Grifoni, A. et al. Targets of T cell responses to SARS-CoV-2 coronavirus in humans with COVID-19 disease and unexposed individuals. *Cell* **181**, 1489–1501.e1415 (2020).
36. Laidlaw, B. J. & Ellebedy, A. H. The germinal centre B cell response to SARS-CoV-2. *Nat. Rev. Immunol.* **22**, 7–18 (2022).
37. Mudd, P. A. et al. SARS-CoV-2 mRNA vaccination elicits a robust and persistent T follicular helper cell response in humans. *Cell* **185**, 603–613.e615 (2022).
38. Cumpelik, A. et al. Dynamic regulation of B cell complement signaling is integral to germinal center responses. *Nat. Immunol.* **22**, 757–768 (2021).
39. Afkhami, S. et al. Respiratory mucosal delivery of next-generation COVID-19 vaccine provides robust protection against both ancestral and variant strains of SARS-CoV-2. *Cell* **185**, 896–915.e819 (2022).
40. Elsner, R. A. & Shlomchik, M. J. Germinal center and extrafollicular B cell responses in vaccination, immunity, and autoimmunity. *Immunity* **53**, 1136–1150 (2020).
41. Robinson, M. J. et al. Long-lived plasma cells accumulate in the bone marrow at a constant rate from early in an immune response. *Sci. Immunol.* **7**, eabm8389 (2022).
42. Baden, L. R. et al. Efficacy and safety of the mRNA-1273 SARS-CoV-2 vaccine. *N. Engl. J. Med.* **384**, 403–416 (2021).

43. Xia, S. et al. Effect of an inactivated vaccine against SARS-CoV-2 on safety and immunogenicity outcomes: interim analysis of 2 randomized clinical trials. *Jama* **324**, 951–960 (2020).

44. Yue, C. et al. ACE2 binding and antibody evasion in enhanced transmissibility of XBB.1.5. *Lancet Infect. Dis.* **23**, 278–280 (2023).

45. Liu, Y. et al. Inactivated vaccine-elicited potent antibodies can broadly neutralize SARS-CoV-2 circulating variants. *Nat. Commun.* **14**, 2179 (2023).

46. Peng, D. et al. Heterologous vaccination with subunit protein vaccine induces a superior neutralizing capacity against BA.4/5-included SARS-CoV-2 variants than homologous vaccination of mRNA vaccine. *MedComm* **4**, e238 (2023).

47. Shen, X. Boosting immunity to Omicron. *Nat. Med.* **28**, 445–446 (2022).

48. Ai, J. et al. Recombinant protein subunit vaccine booster following two-dose inactivated vaccines dramatically enhanced anti-RBD responses and neutralizing titers against SARS-CoV-2 and variants of concern. *Cell Res.* **32**, 103–106 (2022).

49. Haas, E. J. et al. Impact and effectiveness of mRNA BNT162b2 vaccine against SARS-CoV-2 infections and COVID-19 cases, hospitalisations, and deaths following a nationwide vaccination campaign in Israel: an observational study using national surveillance data. *Lancet* **397**, 1819–1829 (2021).

50. Xie, T. et al. Three doses of prototypic SARS-CoV-2 inactivated vaccine induce cross-protection against its variants of concern. *Signal Transduct. Target. Ther.* **7**, 61 (2022).

51. Collier, A. Y. et al. Immunogenicity of BA.5 bivalent mRNA vaccine boosters. *N. Engl. J. Med.* **388**, 565–567 (2023).

52. Chalkias, S. et al. A bivalent Omicron-containing booster vaccine against Covid-19. *N. Engl. J. Med.* **387**, 1279–1291 (2022).

53. Stuart, A. S. V. et al. Immunogenicity, safety, and reactogenicity of heterologous COVID-19 primary vaccination incorporating mRNA, viral-vector, and protein-adjuvant vaccines in the UK (Com-COV2): a single-blind, randomised, phase 2, non-inferiority trial. *Lancet* **399**, 36–49 (2022).

54. Yang, J. et al. A vaccine targeting the RBD of the S protein of SARS-CoV-2 induces protective immunity. *Nature* **586**, 572–577 (2020).

55. Bąchor, R., Kluczyk, A., Stefanowicz, P. & Szewczuk, Z. New method of peptide cleavage based on Edman degradation. *Mol. Divers.* **17**, 605–611 (2013).

56. Gagne, M. et al. mRNA-1273 or mRNA-Omicron boost in vaccinated macaques elicits similar B cell expansion, neutralizing responses, and protection from Omicron. *Cell* **185**, 1556-1571.e1518 (2022).

Author contributions
X.W. conceived and supervised the research and designed the experiments. Z.C., G.L. and J.L. performed gene cloning, expression, and protein purification. X.S. prepared mRNA vaccine design and development. Z.S. performed negative-staining transmission electron microscopy. Jingyun Yang, C.H. and H.L. performed vaccine formulation and vaccinations in mice and performed binding antibodies assay and neutralization of pseudovirus experiment. Jingyun Yang, C.H. and H.L. performed flow cytometry to assay GC B, Tfh, and T cellular immune response. Y.Z. and H.Y. performed authentic SARS-CoV-2 neutralization assay. Youchun Wang, Q.S., S.L., Y.Y., W.Y., C.T., J.W., B.L. and Q.H. performed SARS-CoV-2 challenge in mice and determined the viral loads. H.S., Z.W., and W.L. organized the IIT clinical trial, overseeing administration and sample collection. Jingyun Yang, W.H., C.H., H.L., A.A., J.L., L.Y., W.W., G.S., Jinliang Yang, Z.Z., Yuquan Wei, G.L. and X.W. analyzed, interpreted the data and assisted with the adjustments of directions and interpretation of the mechanical aspects of the results. X.W. and W. H. wrote the manuscript. All authors have read and approved the article.

Competing interests
This work was supported by the WestVac Biopharma Co. Ltd. Jingyun Yang, J.L., L.Y., Z.W., W.W., G.S., Jinliang Yang, Z.Z., Yuquan Wei, G.L., and X.W. are also working at the WestVac Biopharma Co. Ltd. The remaining authors declare no competing interests.

Additional information
Supplementary information The online version contains supplementary material available at https://doi.org/10.1038/s41467-024-55087-z.

Correspondence and requests for materials should be addressed to Qiangming Sun, Shuaiyao Lu, Zhenling Wang, Youchun Wang, Guangwen Lu, Weimin Li or Xiawei Wei.

Peer review information *Nature Communications* thanks Juliana Cassataro, Katrina Pollock and the other, anonymous, reviewer(s) for their contribution to the peer review of this work. A peer review file is available.

Reprints and permissions information is available at http://www.nature.com/reprints

Publisher's note Springer Nature remains neutral with regard to jurisdictional claims in published maps and institutional affiliations.

Jingyun Yang[1,2,7], Weiqi Hong ®[1,2,7], Huashan Shi[1,2,7], Cai He[1,2,7], Hong Lei[1,2,7], Yanan Zhou[3,7], Hao Yang[3,7], Aqu Alu[1,2], Zimin Chen ®[1,2], Yun Yang[3], Wenhai Yu[3], Cong Tang[3], Junbin Wang[3], Bai Li[3], Qing Huang[3], Jiong Li ®[1,2], Li Yang[1,2], Wei Wang ®[1,2], Guobo Shen[1,2], Jinliang Yang[1,2], Zhiwei Zhao[1,2], Xiangrong Song ®[1,2], Zhaoming Su[1,2], Yuquan Wei[1,2], Qiangming Sun ®[3 ✉], Shuaiyao Lu ®[3 ✉], Zhenling Wang ®[1,2 ✉], Youchun Wang[3 ✉], Guangwen Lu ®[1,2 ✉], Weimin Li ®[4,5,6 ✉] & Xiawei Wei ®[1,2 ✉]

[1]Laboratory of Aging Research and Cancer Drug Target, National Clinical Research Center for Geriatrics, West China Hospital, Sichuan University, Chengdu, China. [2]State Key Laboratory of Biotherapy and Cancer Center, West China Hospital, Sichuan University, Chengdu, China. [3]National Kunming High-level Biosafety Primate Research Center, Institute of Medical Biology, Chinese Academy of Medical Sciences and Peking Union Medical College, Kunming, China. [4]Department of Pulmonary and Critical Care Medicine, West China Hospital, Sichuan University, Chengdu, China. [5]Precision Medicine Center, Precision Medicine Key Laboratory of Sichuan Province, West China Hospital, Sichuan University, Chengdu, China. [6]Institute of Respiratory Health, Frontiers Science Center for Disease-related Molecular Network, West China Hospital, Sichuan University, Chengdu, China. [7]These authors contributed equally: Jingyun Yang, Weiqi Hong, Huashan Shi, Cai He, Hong Lei, Yanan Zhou, Hao Yang. ✉e-mail: qsun@imbcams.com.cn; lushuaiyao-km@163.com; wangzhenling@scu.edu.cn; wangyc@imbcams.com.cn; lugw@scu.edu.cn; weimi003@scu.edu.cn; xiaweiwei@scu.edu.cn